https://doi.org/10.5194/egusphere-2026-809
Preprint. Discussion started: 17 February 2026

Atlantic water intrusions onto the Scotian Shelf during the past 8.6 ka BP

Henriette M. Kolling[1], Markus Kienast[†], Peter Matzerath[1], Julia Gottschalk[1], Stephanie Kienast[2], Daniel A. Frick[1], Felix Gross[1, 3], Jack Wharton[4], David Thornalley[4], Ralph R. Schneider[1]

[1] Institute of Geosciences, Kiel University, Ludewig-Meyn-Straße 10, 24118 Kiel, Germany
[†] deceased
[2] Department of Oceanography, Dalhousie University, 1355 Oxford Street, Halifax B3H 4R2 NS, Canada
[3] Center for Ocean and Society, University of Kiel, Kiel, Germany
[4] Department of Geography, University College London, London, UK

Correspondence to: Henriette M. Kolling (henriette.kolling@ifg.uni-kiel.de)

Abstract. The Scotian Shelf lies at the confluence of warm Gulf Stream (GS) waters and the cold Labrador Current (LC), making it highly sensitive to large- and small-scale climate variability. Modern observations show rapid regional warming accelerated by episodic GS-derived intrusions, yet Holocene paleoceanographic reconstructions from this margin are sparse and often conflicting with respect to the frequency and extent of intrusion events. Here, we present high-resolution Mg/Ca-derived sea-surface temperature (SST) and planktonic $\delta^{18}O$ records from St. Anns Basin on the north-eastern Scotian Shelf that provide new insights into the hydrographic surface-ocean variability of the past 8.5 ka calibrated Before Present (cal BP). While the SST record does not capture the 8.2 ka event, this event is evident in the $\delta^{18}O$ and Ca/Sr records, indicating that its freshwater signal reached the Scotian Shelf. Reconstructed SSTs are generally cold from ~8.5 to ~6.2 cal ka BP, followed by a gradual increase in mean SSTs punctuated by multiple short-lived warm and saline events beginning around 6 cal ka BP, at 6.0-5.8, 5.5-5.4, 5.1-4.9, 3.2-3.1, 2.5-2.2 and 1.05-0.8 cal ka BP, which we interpret as intrusions of GS-sourced slope waters. We attribute these events to basin-scale reorganizations of the GS-LC system, consistent with the minimum/maximum modal state framework of Pickart et al. (1999). Minimum modal state circulation, characterized by a strong onshore LC and an intensified Deep Western Boundary Current (DWBC), which is dominated by Denmark Strait Overflow water, creates a sharp front which restricts intrusions of warm water onto the Scotian Shelf. Maximum modal state conditions feature a weakened LC and increased Labrador Sea Water (LSW) contribution to the DWBC, and reduce cross-slope temperature and salinity gradients that permit GS-derived waters to penetrate the shelf. Overall, our results indicate that warm-water intrusions occurred regularly throughout the past 6.5 ka BP with magnitudes of 6.7°C and 1.5 psu comparable to those observed today.

https://doi.org/10.5194/egusphere-2026-809
Preprint. Discussion started: 17 February 2026

1. Introduction

The northwest Atlantic provides a unique environment to monitor and reconstruct modern and past ocean variability, respectively. Within the NW Atlantic, the Scotian Shelf is a critical climatic region as it lies at the frontal zone between the colder and fresher polar waters of the Labrador Current (LC) and warmer and saltier Atlantic water masses from the Gulf Stream (GS) (Fig. 1). Both currents are key components of the Atlantic Meridional Overturning Circulation (AMOC) and are influenced by changes in the Subpolar Gyre (SPG) (Brickman et al., 2018; Gonçalves Neto et al., 2021). Over the past decade, the Scotian Shelf has warmed faster than many other ocean regions (e.g., Pershing et al., 2016). Climate models suggest that present-day and future warming of the water column on the Scotian Shelf is linked to the retreat/retroflection of the LC and a northward shift of the GS (Zhang & Vallis, 2007; Saba et al., 2016). Further, the continuous sea surface temperature (SST) warming trend since 2011 has been linked to increasing GS intrusions onto the Scotian Shelf that was associated with a general northward shift of the GS system (Gonçalves Neto et al., 2021 and references therein). The degree to which these oceanographic changes are influenced by basin-scale processes, including AMOC and SPG dynamics, as well as enhanced freshwater fluxes from melting Arctic sea ice and glaciers, remains uncertain.

Holocene SST reconstructions from the northwest Atlantic off Canada, including the Scotian Shelf (Levac, 2002; Keigwin et al., 2003; Sachs, 2007) are often described as ambiguous due to the strong influence on LC variability, freshwater input, and seasonal or stratification effects. Levac (2002) employed dinocyst transfer functions to reconstruct surface ocean conditions in La Have and St. Anns Basins: La Have Basin shows an early Holocene warming peak (~10.5-8.5 ka BP) followed by middle Holocene cooling, whereas St. Anns Basin exhibits a later early-Holocene peak (~7.5-6 ka BP) and a second warm interval between ~5 and 2.5 ka BP. In the adjacent Emerald Basin, Sachs (2007) recorded a more muted SST signal, with an overall Holocene cooling trend using alkenones. In the same basin, Keigwin et al. (2003) applied Mg/Ca thermometry and stable isotopes on planktonic foraminifera, documenting distinct early-Holocene warmth followed by mid-Holocene cooling. These diverging patterns reflect complex regional interactions between the GS and LC and are further complicated by seasonal biases inherent to different SST proxies (Schneider et al., 2010). Moreover, no high-resolution, continuous Holocene reconstructions exist that capture centennial- to decadal-scale hydrographic variability in the GS-LC system on the Scotian Shelf. Understanding this variability is critical as shifts in the balance between subpolar and subtropical waters in the NW Atlantic may reflect broader oceanographic changes in the NW Atlantic Ocean, controlling the delivery of warm, saline Atlantic waters onto the Atlantic Canadian Shelf (Pickart et al., 1999). Such modal-state transitions influence local SST and sea surface salinity (SSS), and, as shown in terrestrial records, can drive broader hydroclimatic effects in the North Atlantic region (Shuman et al., 2019).

https://doi.org/10.5194/egusphere-2026-809
Preprint. Discussion started: 17 February 2026

In this study, we present a high-resolution Holocene reconstruction of SST and water mass dynamics from the Scotian Shelf using planktonic foraminiferal Mg/Ca thermometry and stable oxygen isotopes. For additional freshwater reconstruction we present elemental data, i.e. Ca/Sr ratio and calcite content. Our record provides new insights into centennial- to millennial-scale variability in the GS-LC system and allows a link to be made from local SST-SSS anomalies to modal-state circulation, AMOC and SPG variability, and broader North Atlantic climate patterns.

1.1. Regional Oceanography

The surface ocean circulation proximal to the Scotian Shelf reflects the competing influence of the LC and the GS, both components of the SPG. On its western boundary, the LC consist of an inner and an outer branch (Fig. 1). The inner LC is fed by outflow from Davis and Hudson Straits, whereas the outer LC is a continuation of the West Greenland Current (Fig. 1; Lazier & Wright, 1993; Straneo & Saucier, 2008). The outer LC follows the shelf edge southward along the coast of Labrador and Newfoundland, feeds the Slope Water Jet along the Scotian Slope, and contributes to the inflow into the Laurentian Channel (Fig. 1; Loder et al., 1998, 2003; Fratantoni & McCartney, 2010). The inner LC flows parallel to the outer LC on the Labrador Shelf until entering the Gulf of St. Lawrence via the Strait of Belle Isle, where it mixes with Gulf of St. Lawrence outflow and continues onto the Scotian Shelf as the Nova Scotia Current (NSC; Fig. 1).

On the southern boundary of the SPG, the GS transports warm, saline and relatively oxygen-depleted waters northwards along the U.S. eastern coast before turning towards the east at Cape Hatteras (~35.2°N). It then meanders northeast towards the Grand Banks of Newfoundland, generating warm eddies which may reach the Scotian Shelf (Brickman et al., 2018). These eddies enter the Scotian Shelf via deep gullies and channels (Petrie & Drinkwater, 1993; Loder et al., 1998; Petrie & Yeats, 2000) and can be considered a key mechanism for episodic intrusions of warm, saline slope waters onto the Scotian Shelf.

The interaction between the cold waters of the LC and the warm, saline GS forms the Slope Waters along the Scotian Slope, which comprise of cold Labrador Subarctic Slope Water and the warm Atlantic Thermal Slope Water (ATSW; Greene et al., 2013; Seidov et al., 2021). At greater depth, the Deep Western Boundary Current (DWBC) carries components of LSW and Denmark Strait Overflow Water (DSOW), both key components of the North Atlantic Deep Water (NADW) (Bower et al., 2009).

The Scotian Shelf exhibits a strong spatial gradient in SST and SSS (Petrie & Drinkwater, 1993). St. Anns Basin (Fig.1) on the northeastern Scotian Shelf modern summer SSTs (0-5m water depth) reach around 3-4°C (World Ocean Atlas 2023; Locarnini et al., 2023) and salinities of 31.5 psu (World Ocean Atlas 2023; Reagan et al., 2023). SST anomalies of up to 2°C have been reported for more than 50 years typically within the upper 150m of the water column (Lauzier, 1965). However more recent observations indicate anomalies of up to 4°C and salinity anomalies of 0.5 psu within the upper 300m water depth in Scotian Shelf Basins (Hebert et al., 2021).

https://doi.org/10.5194/egusphere-2026-809
Preprint. Discussion started: 17 February 2026

2. Material & Methods

2.1. Sediment Material

Gravity core MSM101_44-3 was taken during expedition MSM101 with the German research vessel Maria S. Merian from St. Anns Basin on the north-eastern Scotian Shelf (45°46.651'N 58°31.967'W, Fig. 1) at 274 m water depth (Schneider et al., 2021). Upon recovery, the core was cut into 1 meter-sections, with each section subsequently split lengthwise into a working and archive half. The sediment material consists of olive-greyish to dark greyish-brown, organic-rich, hemipelagic silty clays, with varying degrees of bioturbation. Sediment samples were taken onboard using 10 ml-syringes in 5 cm-intervals and stored at 4°C. They were freeze-dried and washed over 63- and 150 µm-sieves in the sediment laboratories at Kiel University.

2.2. Chronology

The chronology of core MSM101_44-3 is based on 10 accelerator mass spectrometry (AMS) ^{14}C dates of mixed benthic foraminifera obtained at Leibniz Laboratory for Radiometric Dating and Stable Isotope Research at Kiel University (Matzerath et al., 2026). Radiocarbon dates were converted to calendar ages BP and a sediment depth-age model was developed (Fig. 2, Appendix A - Table A1) using a Bayesian Poisson-process deposition model with the software package OxCal v4.4.4. (Ramsey, 2008, 2009) and the Marine20 dataset (Heaton et al., 2020). The local marine reservoir offset was assumed to be -86 (±66) years, based on the Canadian Marine Reservoir Ages database (McNeely et al., 2006; Matzerath et al., 2026). The resulting modelled ages have 95.4% credible interval widths of 350-530 years.

2.3. Mg/Ca measurements and temperature estimates

For Mg/Ca measurements, about 20-50 specimens of the planktonic foraminifera *Neogloboquadrina pachyderma* were picked from the >150 µm size fraction of the sediment. Each sample was gently crushed between two glass plates and subsequently transferred in a pre-cleaned PCR-vial. Foraminifera tests were cleaned following established protocols after Barker et al., (2003). This procedure incorporates an oxidative cleaning step, which includes clay removal by several milli-Q and methanol rinses and organic matter removal with alkali-buffered 1% H_2O_2 solution in a hot water bath (~100°C for 10min). Prior to a final leaching step, using ultrapure 0.001M HNO_3, remaining silicates were removed by hand with a fine brush. Dissolved and diluted samples (0.1 M ultrapure HNO_3) were measured with an inductively coupled plasma-optical emission spectrometry (ICP-OES) instrument (Spectro Arcos) at the Institute of Geosciences at Kiel University. The instrument was calibrated for Ca concentrations between 15 and 30 mg/L. For samples outside this range, a higher degree of uncertainty is expected and they were excluded from the data set. Instrument stability and accuracy were controlled using the reference material ECRM 752-1 (Limestone), with 1.01 % relative standard deviation throughout the measurements (n=20). Additional trace elements (Fe, Al, Mn) were monitored to check for possible contamination originating from authigenic foraminiferal coatings or introduced during the cleaning procedure. For surface water temperature estimates ($SST_{Mg/Ca}$), the calibration of Elderfield & Ganssen (2000) adapted by Jonkers et al. (2013) was used.

https://doi.org/10.5194/egusphere-2026-809
Preprint. Discussion started: 17 February 2026

$$\frac{Mg}{Ca} = 0.687 * e^{0.09*SST}$$

The standard deviation of the Mg/Ca measurements was controlled by 10 duplicate samples and averaged to 0.02 mmol/mol which translates into an average uncertainty of 0.21°C for our SST estimates.

Mn/Ca ratios were measured and evaluated to assess the cleaning efficiency and possible contamination from diagenetic processes. Generally, Mn/Ca ratios are low (< 0.2 mmol/mol) and do not show a significant correlation to Mg/Ca ratios (r^2 = 0.025; p = <0.01, Appendix B - Fig. B1). Based on the protocol of Boyle (1983), the threshold level of 100 µmol/mol for diagenetic coatings is surpassed in 62 of our samples. Hence, we apply a correction based on Elderfield et al. (2012) for all Mg/Ca values. Corrected and uncorrected Mg/Ca data do not differ (Fig. 2), we conclude that Mn-rich authigenic coatings did not significantly bias our planktonic foraminiferal Mg/Ca data.

N. pachyderma abundances in the water column of the Irminger Sea have been shown to peak during spring and late summer phytoplankton blooms, and its $\delta^{18}O$ signal reflects temperatures from below the seasonal mixed layer (Jonkers et al., 2010). More broadly, studies from the Arctic and North Atlantic demonstrate that the depth habitat of *N. pachyderma* varies systematically with sea-ice cover and chlorophyll concentration, with a consistent preference for a depth habitat below the chlorophyll maximum (Greco et al, 2020). Under conditions of strong sea-ice cover and/or high chlorophyll concentrations, the species typically occupies depths of ~50-100 m, whereas under reduced sea-ice cover and lower productivity conditions its depth habitat deepens to ~75 and 150 m (Greco et al., 2020). On the Scotian Shelf, the mixed layer depth is generally ~60-80 m, shoaling to <20m during summer stratification (Colbourne et al., 2015; Renkl et al., 2024), while the chlorophyll maximum is typically located in the upper to mid-euphotic zone at ~20-40m (Herman & Platt, 1986). Taken together, these constraints suggest that the reconstructed SSTs derived from *N. pachyderma* primarily reflect spring-summer subsurface temperatures integrated over approximately 20-80 m water depth.

2.4. Stable oxygen isotopes

For stable oxygen isotope measurements, 25 crushed specimen of *N. pachyderma* were used. Analyses were carried out using a Finnigan MAT 253 mass spectrometer coupled with a Kiel IV carbonate preparation device at Leibniz Laboratory for Radiometric Dating and Stable Isotope Research at Kiel University. All carbonate data are reported in delta notation ($\delta^{18}O_c$) with reference to the Vienna Pee Dee Belemnite (V-PDB) standard. Five duplicate samples resulted in a standard deviation of $\delta^{18}O_c$ =0.13‰. For calculating the $\delta^{18}O$ of seawater ($\delta^{18}O_{sw}$), the measured $\delta^{18}O_c$ (in ‰ V-PDB) was, in a first step, translated to the Vienna Standard Mean Ocean Water (V-SMOW) scale by adding 0.27 ‰. In a second step, the equation of Bemis et al. (1998)

https://doi.org/10.5194/egusphere-2026-809
Preprint. Discussion started: 17 February 2026

$$T = 16.5 - 4.80\ (\delta^{18}O_c - \delta^{18}O_{sw})$$

was applied, where T represents the $SST_{Mg/Ca}$ in our study core. In a last step, $\delta^{18}O_{sw}$ was corrected for global ice volume ($\delta^{18}O_{sw\text{-}ivc}$) by using a sea-level correction of 0.0083‰ per 1 m (Siddall et al., 2003), derived from the relative sea level curve by Austermann et al. (2013).

SSS were calculated based on the global equation by LeGrande & Schmidt, (2006):

$$SSS = (\delta^{18}O_{sw} + 18.98)/0.55.$$

2.5. X-ray fluorescence (XRF) core scanning

Elemental composition of the bulk sediment was determined on the archive halves of core MSM101_44-3 at Kiel University using an Avaatec XRF core scanner. The sediment surface was smoothed and covered with a 4-µm-thin SPEXCertiPrepUltralene foil to avoid contamination during measurements (Richter et al., 2006). Each core section was successively scanned using a 10kV (tube current: 200µA, time: 10s, no filter) and a 30kV (tube current: 800µA, time: 20s, Pd-thick filter). To ensure instrument stability, standard materials (SARM4, JGa-1, JR-1, KGa-1) were measured at the start and end of each analytical day.

2.6. X-ray diffraction (XRD) analyses

For XRD analyses, 40 freeze-dried and homogenised sediment samples were analysed for their main mineral components with X-ray diffraction using a Bruker AXS D 8 Discover equipped with a copper x-ray tube at Kiel University (step size: 0.0037° 2θ, count time: 1.5 s, scan range: 10°-70° 2θ). XRD results were processed using the HighScore Plus Version 4.8. (4.8.0.25518) by PANalytical and the Inorganic Crystal Structure Database (ICSD) from FIZ – Leibniz Institute for Information Infrastructure Karlsruhe. Quantitative mineral phase analysis was performed via automatic Rietveld refinement, in which the software iteratively adjusts the scale factors of the constituents' phases to achieve an optimal least-squares fit between the observed and calculated diffraction patterns, thereby providing robust estimates of the relative mineral abundances. Based on internal calibration, the uncertainties of the Rietveld-derived abundances were estimated to be approximately ±10%.

2.7. Spectral Analysis

For statistical analysis, spectral analysis was performed on time series of $SST_{Mg/Ca}$ reconstructions, $\delta^{18}O_c$ and $\delta^{18}O_{sw\text{-}ivc}$ using the QAnalySeries program version 1.5.4. (Kotov & Pälike, 2018). Each data series was detrended using QAnalySeries (Kotov & Pälike, 2018). Spectral densities were then calculate using the BTuckey function, and the significance of spectral peaks was assessed at the 95% confidence level.

3. Results

https://doi.org/10.5194/egusphere-2026-809
Preprint. Discussion started: 17 February 2026

3.1. Age model

Sediment core MSM101_44-3 represents the past 10 cal ka BP with sedimentation rates ranging between 66 and 134 cm/ka (Fig. 2). Lowest sedimentation rates (66 cm/ka) are observed in the oldest core sections until 7.4 cal ka BP, afterwards sedimentation rates increase rapidly reaching the highest values of the record around 4.8 cal ka BP with 134 cm/ka (Fig. 2). This steep increase is followed by sedimentation rates falling to 104 cm/ka until 2.8 cal ka BP, when the sedimentation rates continue to rise again towards the core top reaching 119 cm/ka BP (Fig. 2). Based on these sedimentation rates and our sample interval of 5 cm, a resolution of 36 – 74 years is reached with our record, adequate to resolve centennial to multi-decadal hydrographic changes in the study region.

3.2. Mg/Ca ratios and $SST_{Mg/Ca}$ estimates

The absence of planktonic foraminifera prior to 8.6 cal ka BP limits the reconstruction of a compete Holocene Mg/Ca record. Between 8.6 and 6.5 cal ka BP, *N. pachyderma* Mg/Ca ratios remain stable around 1.02 mmol/mol, corresponding to an average SST of approximately 0.9°C (Fig. 3). From 6.5 to 3 cal ka BP, Mg/Ca ratios display pronounced variability (0.7-2.6 mmol/mol), yielding reconstructed SSTs between -2.1 and 13.5 °C, with a mean of ~1.2°C (Fig. 3). This high amplitude variability continues through the most recent interval (3 – 0.2 cal ka BP), but around a slightly higher SST baseline of ~3 °C (Fig. 3). During this period, *N. pachyderma* Mg/Ca ratios range 0.7 between 2.8 mmol/mol Mg/Ca, equivalent to SSTs ranging from -1.8 to 9.4 °C and an average SST of 2.5°C (Fig. 3). These temperatures are consistent with modern subsurface conditions on the Scotian Shelf, where temperatures of 0.4-2.8 °C are observed at 20-100m water depth (World Ocean Atlas 2023; Locarnini et al., 2023).

3.3. Stable oxygen isotopes

Planktonic $\delta^{18}O_c$ values exhibit a distinct negative excursion by ~1‰ V-PDB around 8 cal ka BP followed by a stabilization of $\delta^{18}O_c$ values of ~1.8 ‰ V-PDB until 4 cal ka BP (Fig. 3). Between 3.2 and 2.1 cal ka BP, $\delta^{18}O_c$ values decline slightly to 1.6 ‰ before increasing thereafter, reaching 2 ‰ V-PDB at the core top (0.2 cal ka BP) (Fig. 3).

The ice volume corrected oxygen isotope signature ($\delta^{18}O_{sw\text{-}ivc}$), mirrors the $\delta^{18}O_c$, with minimum values around 8 cal ka BP (-2.5 ‰ V-SMOW) and a rise to intermediate values (-2 ‰ V-SMOW) between 6.2 and 2.8 cal ka BP (Fig. 3). From 2.8 cal ka BP onward, $\delta^{18}O_{sw\text{-}ivc}$ values decreases again to an average of -1.5 ‰ V-SMOW until the core top (Fig. 3). Several distinct positive excursions in $\delta^{18}O_{sw\text{-}ivc}$ occur at ~6.0, 5.0, 2.2 and 1.0 cal ka BP (Fig. 3).

3.4. Elemental composition

XRF Ca/Sr ratios decrease throughout the core, with higher values in the older sediments and lower values after ~4 cal ka BP (Fig. 3). A pronounced XRF Ca/Sr peak occurs between 8.7 and 8.3 cal ka BP (Fig. 3). XRD Calcite content follows a broadly similar pattern, decreasing gradually from ~7 wt% until approximately 6 ka cal BP to ~3 wt% towards the core top (Fig. 3). A

https://doi.org/10.5194/egusphere-2026-809
Preprint. Discussion started: 17 February 2026

distinct maximum, reaching up to 10 wt% calcite, is recorded between 8.5 and 8.1 cal ka BP, coinciding with the XRF Ca/Sr peak at that time (Fig. 3). Generally, XRF Ca/Sr and XRD Calcite content follow the same trend.

4. Discussion

4.1. Holocene hydrographic evolution on the Scotian Shelf

Our new $SST_{Mg/Ca}$ record indicates relatively stable temperatures with a slight warming trend over the past 8.6 cal ka BP (Fig. 3F and 4A). Superimposed on this trend, several distinct warm anomalies occur within the past 6.5 cal ka BP (Fig. 3F). This aligns with dinocyst-based reconstructions (Fig. 4; Levac, 2001, 2002) but contrasts with other micropaleontological (Scott et al., 1984; Orme et al., 2021) and alkenone-based SST (Fig. 4; $SST_{Alkenone}$; Sachs, 2007) reconstructions from the Scotian Shelf. Similar discrepancies between $SST_{Mg/Ca}$ and $SST_{Alkenone}$ proxies have also been reported from the Laurentian Fan (Keigwin et al., 2005). In addition, our record does not show the mid-Holocene warming observed elsewhere in the NW Atlantic between 10 and 6 cal ka, which is typically interpreted as a northward shift of the GS (Fillon, 1976; Vilks & Rashid, 1976; Balsam, 1981; Keigwin & Jones, 1995; Solignac et al., 2004). The absence of such a surface-ocean warming at our study site in St. Anns Basin may be caused by (i) a lack of data prior to 8.5 ka cal BP, (ii) lower relative sea level (Vacchi et al., 2018), partly exposing the shelf-edge sills, likely restricting exchange with the open Atlantic, causing basins to be more isolated, or (iii) a persistent influence of cold meltwater from the Gulf of St. Lawrence throughout the late and mid-Holocene on the Scotian Shelf (Licciardi et al., 1999).

$SST_{Alkenone}$ reconstructions from the Scotian Shelf indicate an overall cooling trend of up to 10°C over the past 10 cal ka BP without any centennial-to-millennial-scale variability (Fig. 4; Sachs, 2007), quite different from the Mg/Ca based SST reconstruction presented here (Fig. 3F). Although alkenone-based reconstructions typically represent ocean temperatures at shallower water depths than *N. pachyderma* or dinocysts (Müller et al., 1998; Herbert, 2001), depth-habitat differences alone cannot explain the contrasting proxy trends, as all proxies record temperatures from a relatively narrow depth range (0-100m), too limited to experience the magnitude of change implied by the differing signals (Wharton, 2022). Comparable $SST_{Alkenone}$ records from the NW Atlantic show similar long-term cooling trends as was observed here (e.g., Keigwin et al., 2005; Marsicek et al., 2018). It was suggested that $SST_{Alkenone}$ reconstructions may reflect GS-LC frontal migration rather than mean seasonal or annual SSTs in the NW Atlantic (Osman et al., 2021). In contrast, alkenone records highlight an extension of the bloom season through the Holocene relative to foraminiferal proxies, with blooms shifting from being restricted to summer to occurring from spring through autumn, which likely contributed to the general cooling trend observed in $SST_{Alkenone}$ records (Keigwin et al., 2005; Eynaud et al., 2018; Bova et al., 2021). Because foraminiferal $SST_{Mg/Ca}$ primarily record spring-summer conditions, which we assume remained relatively consistent throughout our record, our $SST_{Mg/Ca}$ reconstruction provides a complementary perspective to alkenone SSTs, which are influenced by changes in bloom seasonality and/or frontal migration, allowing us to resolve variability not captured by the $SST_{Alkenone}$ records while remaining consistent with broader regional trends.

https://doi.org/10.5194/egusphere-2026-809
Preprint. Discussion started: 17 February 2026

$SST_{Mg/Ca}$ reconstructions extend only as far back as 8.6 cal ka BP, as earlier intervals lack sufficient planktonic foraminifera for reliable analysis (Matzerath et al., 2026). This limitation, attributed to their absence or low abundance, is a well-documented issue on the Scotian Shelf (Scott et al., 1984; Levac, 2002), which may be linked to a shift from sympagic to pelagic conditions around 8.4 cal ka BP at St. Anns Basin due to rising sea level and reduced melt water influence from the Gulf of St. Lawrence (Matzerath et al., 2026).

Our $SST_{Mg/Ca}$ record suggests relatively stable SSTs of around 2°C between 8.5 and 6.5 cal ka BP (Fig. 3). These results agree with dinocyst and sea-ice biomarker reconstructions from St. Anns and La Have Basins, which document a mid-Holocene cooling between 8.7 and 7.0 ka cal ka BP, characterized by lower SSTs and SSSs than today and an extended sea ice period (Fig. 4; Levac, 2002; Matzerath et al., 2026). Planktonic foraminiferal faunal reconstructions and stable oxygen isotopes from Emerald Basin show a similarly pronounced cooling between 8 and 6 cal ka BP (Wharton, 2022). This cooling has been associated with a shift in surface circulation in the North Atlantic due to a SPG contraction which caused a westward shift in the subpolar front, increasing the influence of LC waters on the Scotian Shelf (Fig. 5; Bersch, 2002; Holliday et al., 2020; Yang & Piper, 2021). Together, these findings suggest that the mid-Holocene cooing observed in our $SST_{Mg/Ca}$ record reflects the combined effects of circulation changes and extended sea-ice cover.

This regional cooling aligns with large-scale changes in North Atlantic circulation. A pronounced reduction in NADW ventilation between 8.5 and 6.5 cal ka BP suggest a weakened AMOC during this interval (Oppo et al., 2003 Gerber et al, 2025; Fig. 5). Additional evidence indicates that the LSW component of the NADW was particularly suppressed, implying reduced convection in the Labrador Sea and enhanced upper-ocean stratification (Hillaire-Marcel et al., 2007; Thornalley et al., 2009; Fig. 5). In combination, enhanced stratification of the water column, and a strong, on-shore LC would have prevented Atlantic water intrusions onto the Scotian Shelf, maintaining the relatively stable and cold conditions reflected in our record at St. Anns Basin throughout the last 8.5 ka. Superimposed on this cold early Holocene background, the 8.2 ka event represents a short-lived freshwater perturbation whose expression differs across proxies.

4.2. The 8.2 ka event: Expression on the Scotian Shelf

Planktonic $\delta^{18}O_c$ anomalies and increased detrital carbonate content between 8.5 and 7.9 cal ka BP indicate a meltwater pulse, coinciding with elevated sedimentary inorganic calcite (Fig. 3). This interval likely corresponds to the 8.2 ka cold event, attributed to the catastrophic drainage of Lake Agassiz via Hudson Strait (Lochte et al., 2019). The 8.2 ka cold event is well-documented in terrestrial, marine and ice-core records throughout the Northern Hemisphere (Spooner et al., 2002; Alley & Ágústdóttir, 2005; Rohling & Pälike, 2005). $\delta^{18}O_{sw\text{-}ivc}$ and reconstructed salinities do not record a contemporaneous signal; however, these proxies contain a data gap over this interval (Fig. 3). Despite this, the $\delta^{18}O_c$ and detrital carbonate anomalies provide robust evidence of the meltwater event, consistent with independent Holocene paleoclimate records.

https://doi.org/10.5194/egusphere-2026-809
Preprint. Discussion started: 17 February 2026

Previous studies suggest that the final Lake Agassiz outburst reached the Scotian Shelf, dramatically reducing sea surface salinities (Scott et al., 1984; Levac et al., 2001; Levac, 2002). This freshwater pulse likely became entrained in the GS, significantly impacting AMOC strength (Keigwin et al., 2005) and contributing to the widespread 8.2 ka cold event in the North Atlantic region (Thomas et al., 2007; Hoffman et al., 2012; Jennings et al., 2015; Lochte et al., 2019). A comparable signal in $SST_{Mg/Ca}$ and planktonic $\delta^{18}O$ records from the Laurentian Fan has been reported between 8.4 and 8 cal ka BP (Fig. 4; Keigwin et al., 2005). Reconstructions from the NW Atlantic show a similar $\delta^{18}O$ depletion around ~7.5 cal ka BP (Keigwin & Jones, 1995; de Vernal & Hillaire-Marcel, 2006), which recalibrates to ~8.2 cal ka BP using the Marine20 calibration curve and updated local reservoir corrections based on McNeely et al., (2006). However, some NW Atlantic records lack a clear meltwater signal (e.g., Piper et al., 2021; Rashid et al., 2017), likely due to the strong influence of the cold and fresh LC, which muted expression of the meltwater signal in the sedimentary record (Wharton, 2022).

The absence of a significant SST reduction in relation to the 8.2 ka event in our Mg/Ca record likely reflects pre-existing cold conditions on the Scotian Shelf, driven by the combined influence of a strong LC, persistent freshwater input from the Gulf of St. Lawrence, and seasonal sea-ice cover (Matzerath et al., 2026). Under these already cold and fresh conditions, the upper water column was already at low temperatures, such that additional cooling associated with the 8.2 ka event would have had negligible impact on the $SST_{Mg/Ca}$ signal. Model simulations suggest a salinity reduction of ~5 psu in the subtropical North Atlantic between 8.16-8.74 ka BP (Condron & Winsor, 2011), falling below the tolerance threshold of planktonic foraminifera (e.g., Greco et al., 2020). The *N. pachyderma* specimens found in our core may have adapted by migrating to deeper, more stable water masses – an ecological response consistent with previous studies during the 8.2 ka event (e.g., Simstich et al., 2003). There is no clear evidence for the depth extent of the freshwater pulse that is associated with the 8.2 ka event. Meltwater penetrated the water column of the northern Labrador Shelf, near its source, to depths up to ~200m (Lochte et al., 2019). The depth habitat of *N. pachyderma* on the Scotian Shelf, further south, is difficult to constrain; however, it is likely that during this event, the species calcified at greater depth than during the rest of the record, potentially exceeding 100m.

An alternative explanation could involve freshwater and detrital carbonate input from the Gulf of St. Lawrence region, which contains carbonate outcrops on Anticosti Island (Loring & Nota, 1973). However, evidence for meltwater routing in this area is sparse (Keigwin et al., 2005; Levac et al., 2011) and it is generally accepted that the Gulf of St. Lawrence region was fully deglaciated by ~10.85 cal ka BP (Dyke, 2004).

Between 8.5 and 7.9 cal ka BP, we propose that low SSTs in St. Anns Basin result from a more onshore pathway of the LC, as observed in the NW Atlantic during the early Holocene (Wharton, 2022) coupled with the presence of seasonal sea ice conditions (Matzerath et al., 2026) and significant meltwater inflow from the retreating Laurentide Ice Sheet. The 8.2 ka BP

https://doi.org/10.5194/egusphere-2026-809
Preprint. Discussion started: 17 February 2026

freshwater pulse reached the St. Anns Basin, and caused planktonic foraminifera to migrate to deeper water masses, which explains the occurrence of inorganic calcite along with the discrepancy in $\delta^{18}O_c$ and $SST_{Mg/Ca}$.

4.3. Emergence of mid- to late Holocene hydrographic variability

After ~6.5 cal ka BP, the previously stable cold and relatively fresh sea surface conditions at St. Anns Basin transition to slightly higher SSTs accompanied by a marked increase in variability (Fig. 3). This shift marks the onset of episodic warm and saline anomalies superimposed on a generally cool baseline state (Fig. 3).

Comparable increases in SST variability after ~6.5 cal ka BP have been identified in Emerald Basin based on *N. pachyderma* occurrence, suggesting that this shift reflects broader reorganizations of shelf hydrography (Wharton, 2022). The timing of this transition broadly parallel the establishment of the modern North Atlantic circulation system, characterized by deep water formation in the Labrador Sea after meltwater stratification decreased (Hillaire-Marcel et al., 2001; Born & Levermann, 2010). This reorganization likely weakened the dominance of cold, fresh LC waters on the Scotian Shelf and increased the influence of warmer, saltier Atlantic-sourced waters, leading to the higher and more variable SST and SSS observed in our record.

A modest warming centered around ~6.5 cal ka BP may reflect a short-lived mid-Holocene thermal maximum previously identified on the Scotian Shelf between ~7.5 and 6 cal ka BP in dinocyst records (Fig. 4; Levac, 2002) and supported by pollen-based reconstructions indicating warmer-than-present summer air temperatures in Atlantic Canada (Jetté & Mott, 2007). However, this interpretation contrasts with evidence for a general cooling trend between ~6 and 4 cal ka BP across the NW Atlantic, including *N. pachyderma* occurrence from Emerald Basin (Fig. 4; Wharton, 2022). The relative low baseline SSTs in the St. Anns Basin record (~2.1 °C) suggest that any mid-Holocene warming was weak or regionally muted. This regional cooling has been linked to a contraction of the SPG and a westward shift of the Polar Front, as inferred from both the North Atlantic and the Nordic Seas (Colin et al., 2010; Staines-Urías et al., 2013).

Following ~6.5 cal ka BP, surface-water variability on the Scotian Shelf increases progressively, consistent with evidence for a recovery and strengthening of NADW formation following the early Holocene ventilation minimum (Oppo et al., 2003). The mid-Holocene stabilization of deep-water formation is thought to reflect the waning influence of Laurentide meltwater (de Vernal & Hillaire-Marcel, 2008) and a progressive increase in surface-water density in the Labrador Sea (Thornalley et al., 2009). Such changes would have supported a stronger overturning circulation and a re-expansion of the SPG (Hillaire-Marcel et al., 2001). These large-scale adjustments would have reduced the strong upper-ocean stratification characterizing our study site in the early Holocene and allowed for episodic intrusions of Atlantic sourced warm waters, such as the GS sourced slope waters, after ~6.5 cal ka BP. This interpretation is further supported by increased variability in planktonic $\delta^{18}O$ values after ~6.5 cal ka BP (Fig, 3), indicating more dynamic temperature–salinity conditions and enhanced water-mass variability at the core site.

https://doi.org/10.5194/egusphere-2026-809
Preprint. Discussion started: 17 February 2026

Between 4.4 and 3.2 cal ka BP, our record indicates a relatively stable phase of low SST and SSS. Dinocyst evidence from St. Anns Basin find relatively low summer SSTs, while winter SSTs increased (Fig. 4; Levac, 2002) – nevertheless this is inconsistent with our spring/summer SST reconstruction. Increasing sea ice in the Gulf of St. Lawrence (Solignac et al., 2011) and reduced Atlantic water input to the LC associated with stronger mixing and a weaker SPG likely also contributed to the cold, stable conditions on the Scotian Shelf from 4.4 to 3.2 cal ka BP (Thornalley et al., 2009; Fig 4). However, other hydrographic reconstructions from the NW Atlantic, find a warmer phase at that time associated with a reduction of sea-ice and meltwater export from the Arctic (Fig. 4; Levac, 2002; Solignac et al., 2011; Sheldon et al., 2016).

During the last 3.2 cal ka BP, our record is characterized by lower-amplitude SST variability (Fig. 3F, 4A). This is consistent with foraminiferal assemblages from Emerald Basin, indicating alternating but muted influence of contrasting water masses on the central Scotian Shelf (Fig. 4; Wharton, 2022). This trend may be related to a stabilization of the atmospheric circulation towards the establishment of dominating north-westerly winds in the NW Atlantic region, which also stabilized the GS-LC frontal system (Sheldon et al., 2016).

4.4. Warm water anomalies as indicators of Gulf Stream-sourced slope water intrusions

Superimposed on the mid- to late Holocene trend, the St. Anns Basin record contains several distinct warm and saline anomalies (Fig. 3, 4). In this study, warm events are defined as either extreme events, characterized by at least two consecutive data points exceeding two standard deviations (2σ), or as moderate events, defined by values exceeding one standard deviation (1σ), above the mean SST (2.4°C) and SSS (32 psu). Two peaks consisting of only one data point at 4.7 and 4.5 cal ka BP are excluded. Our record indicates four extreme events from 6.0-5.8, 5.5-5.4, 3.2-3.1 and 2.5-2.2 cal ka BP as well as two moderate warm events from 5.1-4.9 and 1.05-0.8 cal ka BP, which last 100-300 years (Fig. 3). These events are expressed by concurrent positive anomalies in SST and SSS and are superimposed on otherwise cool baseline conditions (Fig. 3).

Although, variations in Mg/Ca ratios can be influenced by factors other than temperature, including pH, calcification depth, or changes in depth habitat due to stratification or oxygenation (Nürnberg et al., 1996; Lea et al., 1999; Simstich et al., 2003; Kuroyanagi & Kawahata, 2004) the warm evens identified here are supported by a coherent SST-SSS signal. This combined temperature-salinity expression provides a robust basis for distinguishing genuine hydrographic anomalies from proxy specific artefacts.

The six SST and SSS anomalies in our St. Anns Basin record after 6.5 cal ka BP most likely reflect episodic intrusions of GS-sourced slope waters. Comparable events have been interpreted in both modern and paleoceanographic studies from the Scotian Shelf as periods of enhanced GS influence and reduced LC strength (Fig. 5; e.g., Keigwin et al., 2005; Townsend et al., 2015; Saba et al., 2016; Gonçalves Neto et al., 2021; New et al., 2021; Jutras et al., 2022). GS-sourced slope waters enter the Scotian

https://doi.org/10.5194/egusphere-2026-809
Preprint. Discussion started: 17 February 2026

Shelf primarily through a limited number of deep gullies and channels incising the Scotian Shelf, e.g., the Gully or the Scotian Gulf (Fig 1; Petrie & Drinkwater, 1993; Loder et al., 1998; Petrie & Yeats, 2000). The origin of these warm waters remains uncertain. They may represent (i) GS-sourced slope waters entering the shelf via the Gully and adjacent channels, or (ii) shallower GS eddies affecting the surface waters only (Silver et al., 2023). Both pathways could have been modulated through post-glacial isostatic uplift. The apparent discrepancy between geochemical evidence for warm intrusions in the NE Scotian Shelf and the absence of such signals in Emerald Basin foraminiferal assemblage-based reconstructions (Fig. 4) likely reflects differences in basin geometry, water-mass pathways, and proxy sensitivity. St. Anns Basin is more sensitive to episodic subsurface Atlantic-derived intrusions that can be recorded by $\delta^{18}O$ and Mg/Ca at specific depth habitats, whereas Emerald Basin assemblages integrate surface conditions over longer timescales and may remain dominated by Labrador Current waters. As a result, transient or subsurface warming events may be effectively masked in assemblage-based SST reconstructions from Emerald Basin.

4.5. Mechanisms controlling modal-state variability

Warm-water intrusions onto the Newfoundland Shelf have been explained by the interaction of the LC, the Slope Water Jet (SJ) and the DWBC (Pickart et al., 1999). Adapting this concept to the Scotian Shelf, we consider two contrasting circulation states that may explain warm-water intrusions to the study site (Fig. 6). During the minimum modal state, a strong onshore LC and an intensified SJ deliver cold, fresh subpolar water masses southward along the slope. At depth, a vigorous DWBC – dominated by cold DSOW – reinforces this configuration, maintaining a sharp front between cold LC and warm GS waters that acts as a barrier to intrusions of warm, saline slope waters. The Scotian Shelf and Slope are therefore dominated by cold, fresh subpolar water masses (Fig. 6). By contrast, during the maximum modal state, reduced LC and SJ strength together with diminished DSOW export and increased LSW influence, flatten the density gradients across the Scotian Slope and allow warm, saline slope waters to intrude onto the shelf (Fig. 6).

Larger scale climate patterns support this interpretation. Shuman et al. (2019) showed that Holocene hydroclimate in the NE United States responded to changes in the North Atlantic temperature gradient: cool subpolar conditions, associated with a steep temperature gradient, produced widespread droughts, whereas warm subpolar conditions, associated with a weaker temperature gradient between the Greenland and the NW Atlantic margin, resulted in wetter intervals. This mirrors the warm SST events during the past 6.5 ka inferred in our Mg/Ca record – periods without warm intrusions on the Scotian Shelf correspond generally to drought events (Fig. 5).

Several large-scale forcing mechanisms may drive these modal shifts. In the modern North Atlantic, positive phases of the North Atlantic Oscillation (NAO; the seesaw in atmospheric pressure between Icelandic Low and Azores High) are associated with enhanced wind stress curl over the subpolar North Atlantic, promoting SPG contraction and a northward displacement of the GS, conditions that favor maximum-mode intrusions (Pickart et al., 1999; Bersch, 2002; Holliday et al., 2020). Conversely,

https://doi.org/10.5194/egusphere-2026-809
Preprint. Discussion started: 17 February 2026

negative NAO phases tend to reinforce minimum modal state conditions. However, the NAO primarily reflects wintertime atmospheric variability and operated on interannual to decadal timescales, limiting its direct application to centennial-to-millennial Holocene records.

Longer-term changes in ocean circulation may therefore provide a more appropriate framework for interpreting the observed modal variability. A weakening of the AMOC has been suggested to shift the GS northward and enhance the influence of subtropical Atlantic slope waters along the NW Atlantic (Zhang & Vallis, 2007; Zhang, 2008; Saba et al., 2016; Caesar et al., 2018). In parallel, SPG-dynamics – controlled by wind stress, and buoyancy forcing – exert additional regional control: a contracted SPG weakens the LC and promotes warm intrusions, while an expanded SPG strengthens subpolar export and reinforced minimum-modal state conditions (Bersch, 2002; Thornalley et al., 2009; Peterson et al., 2017; Holliday et al., 2020).

Together, these processes describe a spectrum of processes capable of shifting the NW Atlantic between minimum (cold, fresh, LC-dominated) to maximum (warm, saline, ATSW intrusions) modal states seen on the Scotian Shelf. Rather than reflecting control by a single driver, maximum modal state intrusions likely occur when multiple conditions align, including reduced LC strength associated with SPG contraction and intervals of weakened AMOC. Reconstructed AMOC minima between 6 and 5 cal ka BP and near 2.8 cal ka BP (Oppo et al., 2003; Fig. 5) may therefore represent background states favorable for enhanced slope-water influence, potentially explaining the cluster of warm events between 6 and 5 ka BP in the St. Anns Basin. The cool anomaly at ~2.8 ka BP suggests that regional circulation patterns, such as sustained subpolar export or persistent LC influence, could locally override the effects of large-scale overturning variability.

The influence of the NAO on the Holocene oceanography of the Scotian Shelf thus remains ambiguous. While instrumental data show correlations between NAO and regional hydrographic variability (Petrie & Drinkwater, 1993; Marsh et al., 1999; Bersch, 2002; Petrie, 2007; Gonçalves Neto et al., 2021), the spatial heterogeneity of NAO impacts and its seasonal focus on winter conditions limit its relevance for our spring-summer proxy record resolving centennial to millennial trends (deMenocal et al., 2000; Orme et al., 2021).

In summary, the centennial-to-millennial-scale hydrographic variability observed in the St. Anns Basin record is best explained by repeated shifts between Pickart-type modal states, driven by low-frequency variability in AMOC strength and SPG geometry, and modulated regionally by changes in LC intensity. These shifts are expressed as episodic intrusions of warm, saline Atlantic slope waters onto the Scotian Shelf when large-scale and regional circulation conditions align.

4.6. Cyclicity of SST variability

Spectral analysis of our SST and SSS record reveals centennial- to millennial-scale cyclicity during the past 8.6 cal ka BP. The most prominent is a 1400-1200-year cycle (Fig. 7), which broadly consistent with the widely recognized ~1500 year oscillation

https://doi.org/10.5194/egusphere-2026-809
Preprint. Discussion started: 17 February 2026

commonly linked to solar forcing (Bond et al., 2001). This mode has frequently been used to explain centennial-to-millennial-scale climate variabilities across the North Atlantic (Haigh, 1996; Swingedouw et al., 2011; Moffa-Sánchez & Hall, 2017) and similar periodicities have been reported in marine and terrestrial records from the NW Atlantic region (Solignac et al., 2004; Willard et al., 2005), including the Scotian Shelf (Levac, 2002).

In our dataset, warm SST-SSS phases generally anti-correlate with Bond events 0, 1, 3 and 5 (~400yrs BP, 1.4 ka BP, 4.2 ka BP, 8.1 ka BP respectively; Fig. 7). Bond events are associated with enhanced drift-ice export, reduced NADW formation, and colder, fresher surface conditions in the Labrador Sea (Bond et al., 2001). Intensified northerly winds during these cold intervals in our record strengthen the LC (Morison et al., 2012) and push the GS-LC frontal zone southward favouring the delivery of cold, fresh subpolar waters to the Scotian Shelf. This circulation pattern closely resembles the minimum modal state described earlier (Pickart et al., 1999), in which a strong LC and an intensified DWBC act as a barrier to the northward penetration of warm, saline Atlantic waters. Hydrographic changes in the St. Anns Basin are consistently associated with Bond events 0, 1, 3 and 5, whereas Bond events 2 and 4 leave no discernible imprint in the record (Fig. 5). This contrast suggest that regional oceanographic conditions modulate whether Bond-scale climate perturbations are expressed on the Scotian Shelf. Before 6 ka BP, the relationship between Bond cycles and our SST-SSS record becomes less consistent, likely due to stronger local oceanographic influences driven by lower relative sea level (Vacchi et al., 2018), enhanced meltwater discharge from the Gulf of St. Lawrence (Licciardi et al., 1999), and an overall colder background state.

We also identify a 200-300-year cycle, consistent with the de Vries solar cycle (Vasil'ev et al., 1999; Muscheler et al., 2003) and a broader ~800-year periodicity that may represent a modulation of the de Vries cycle, consistent with findings from NE Newfoundland (Orme et al., 2021). These longer, solar-paced oscillations could influence the coupling between LC, SJ and the DWBC – the same dynamical system characterizing the minimum-maximum modal state transitions. For instance, periods of reduced solar irradiance are associated with SPG expansion, leading to enhanced subpolar export and a strengthened LC flow (Wanamaker et al., 2008; Moffa-Sánchez et al., 2014), again favoring minimum modal state circulation and cold conditions on the Scotian Shelf. Conversely, periods of enhanced solar output may reduce high-latitude buoyancy forcing and cyclonic circulation in the SPG, leading to SPG contraction and diminished southward subpolar export. The resulting weakening of the LC facilitates Atlantic slope water intrusions, promoting maximum modal state conditions.

Short-period climate oscillations such as the NAO cannot be resolved in this record and are therefore not considered further. However, their known present influence on SPG and LC dynamics provides a useful conceptual framework for understanding how higher-frequency atmospheric variability may interact with lower-frequency oceanic forcing.

Overall, the SST-SSS variability on the Scotian Shelf reflects a combination of externally paced solar forcing and the internal ocean-atmosphere feedbacks that govern modal-state transitions in Northwest Atlantic circulation. Warm phases likely

https://doi.org/10.5194/egusphere-2026-809
Preprint. Discussion started: 17 February 2026

correspond to episodes of weakened LC flow, reduced DWBC transport, and northward GS displacement – conditions characteristic of the maximum modal state, which favor intrusions of Atlantic slope waters into our study region. Cold phases, particularly those aligning with Bond Events, likely reflect minimum modal state configurations characterized by stronger LC influence and enhanced subpolar control. While our results suggest that solar forcing appears to pace millennial- and centennial-scale oceanographic variability on the Scotian Shelf, fully resolving the interplay between solar cycles, NAO/SPG dynamics, and AMOC strength will require higher-resolution and spatially integrated paleoclimate records across the broader Scotian Shelf region.

5. Conclusions

Our new *N. pachyderma* Mg/Ca-derived SST and $\delta^{18}O$ records from the Scotian Shelf provide improved constraints on variability in surface-ocean hydrography over the past 8.6 cal ka BP. Prior to 6.5 cal ka BP, our data indicate cold and fresh surface conditions consistent with continued Laurentide Ice Sheet decay and elevated meltwater discharge through Hudson Strait and the Gulf of St. Lawrence. A distinct freshwater anomaly that we attribute to the 8.2 ka BP event demonstrates that the meltwater reached the NE Scotian Shelf at that time.

During the mid- and late Holocene, SSTs exhibit a modest long-term rise punctuated by multiple warm, saline excursions at 6.0–5.8, 5.5–5.4, 5.1–4.9, 3.2–3.1, 2.5–2.2, and 1.05–0.8 cal ka BP. We interpret these short-lived events as intrusions of GS–sourced slope waters, driven by reorganizations of the GS–LC system. The occurrence of these warm-water intrusions is consistent with alternation between the minimum and maximum modal states defined by Pickart et al., (1999): the minimum modal state, with a strong onshore Labrador Current and DWBC that is dominated by Denmark Strait Overflow Water, suppresses the penetration of warm-water onto the Scotian Shelf, whereas the maximum modal state, marked by a weakened Labrador Current and enhanced contribution of LSW to the DWBC, facilitates intrusions of warm waters onto the Scotian Shelf by reducing cross-slope density gradients.

Overall, our findings indicate that warm-water intrusions comparable in magnitude to modern events were a persistent feature of the Holocene, modulated by variability in AMOC strength, SPG dynamics and multi-centennial solar forcing. Further work is required to determine the spatial extent, sources and forcing mechanisms of these intrusions. Ultra-high-resolution sampling, combined with records from multiple shelf–slope locations, will be critical for determining the impact of NAO-scale variability on Scotian Shelf hydrography and for placing these regional changes within the context of broader North Atlantic circulation modes.

https://doi.org/10.5194/egusphere-2026-809
Preprint. Discussion started: 17 February 2026

Figures

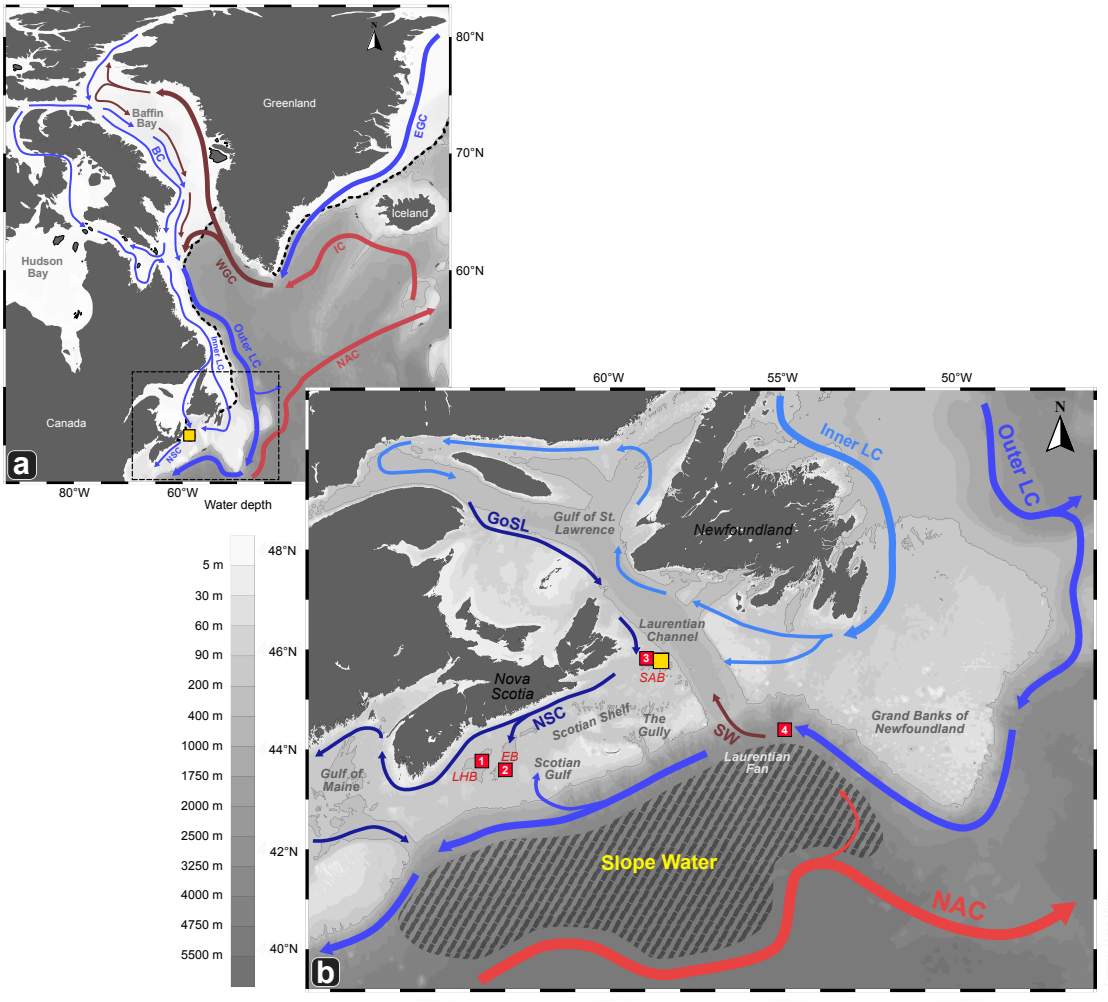

Figure 1: Schematic surface circulation of the NW Atlantic. (a) **The main surface circulation system in the Northwest Atlantic (adapted from Drinkwater, 1996). Blue arrows mark the flow pattern of cold-water surface currents (BC: Baffin Current; EGC: East Greenland Current; LC: Labrador Current; NSC: Nova Scotian Current), while red arrows symbolize the transport of warm surface water masses (WGC: West Greenland Current; IC: Irminger Current; NAC: North Atlantic Current).** (b) **Nova Scotia and Newfoundland Shelves and Slopes bathed by Slope Waters as a result of converging warm and cold-water masses originating from the GS and the LC; NSC: Nova Scotian Current, GoSL: Gulf of St. Lawrence waters, NAC: North Atlantic Current, SW: Slope Water inflow (adapted from Drinkwater, 1996; Brickman et al., 2018). The major sedimentary basins on the Scotian Shelf are the St. Anns Basin (SAB), the Emerald Basin (EB) and the La Have Basin (LHB). The yellow square indicates the core location of this study, MSM101_44-3. Cores mentioned in this study are indicated by red squares, 1: 95-030-24 (Levac, 2001); 2: OCE326-GGC30 (Sachs, 2007; Wharton, 2022); 3: 84-011-12 (Levac, 2002); 4: OCE326-GC26 (Keigwin et al., 2005). Figure adapted from Matzerath et al. (2026).**

https://doi.org/10.5194/egusphere-2026-809
Preprint. Discussion started: 17 February 2026

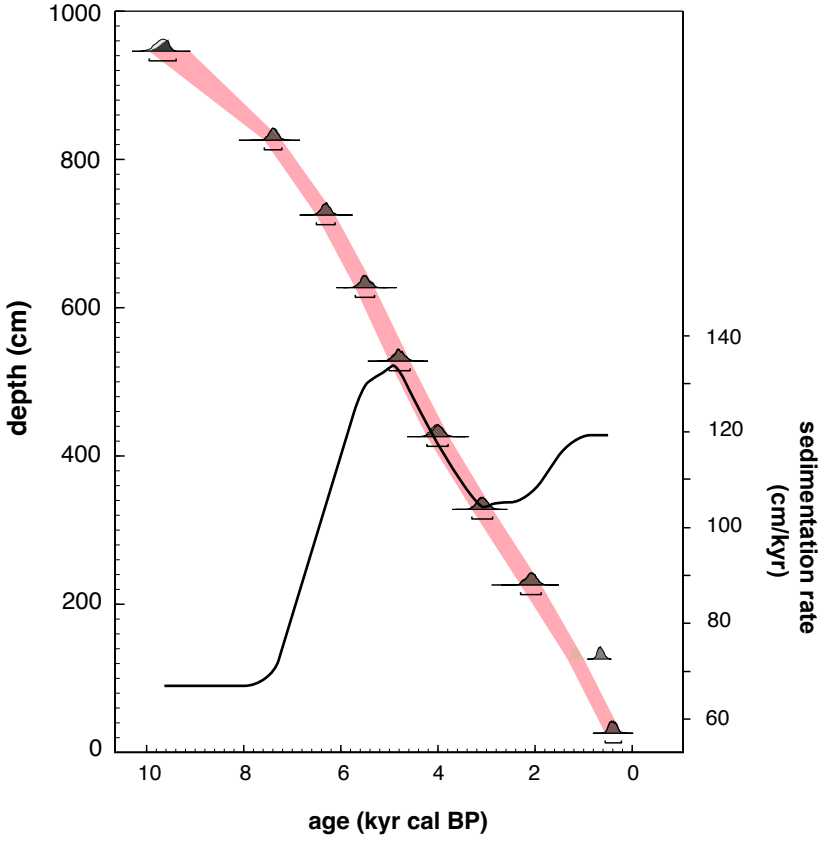

Figure 2: Bayesian age-depth model based on 10 radiocarbon dates (Appendix A - Table A1) for sediment core MSM101_44-3 as published by Matzerath et al. (2026). The red shading indicates the extend of the 95% confidence interval as determined by OxCal. Sedimentation rate is shown in the bottom right (black line).

555

https://doi.org/10.5194/egusphere-2026-809
Preprint. Discussion started: 17 February 2026

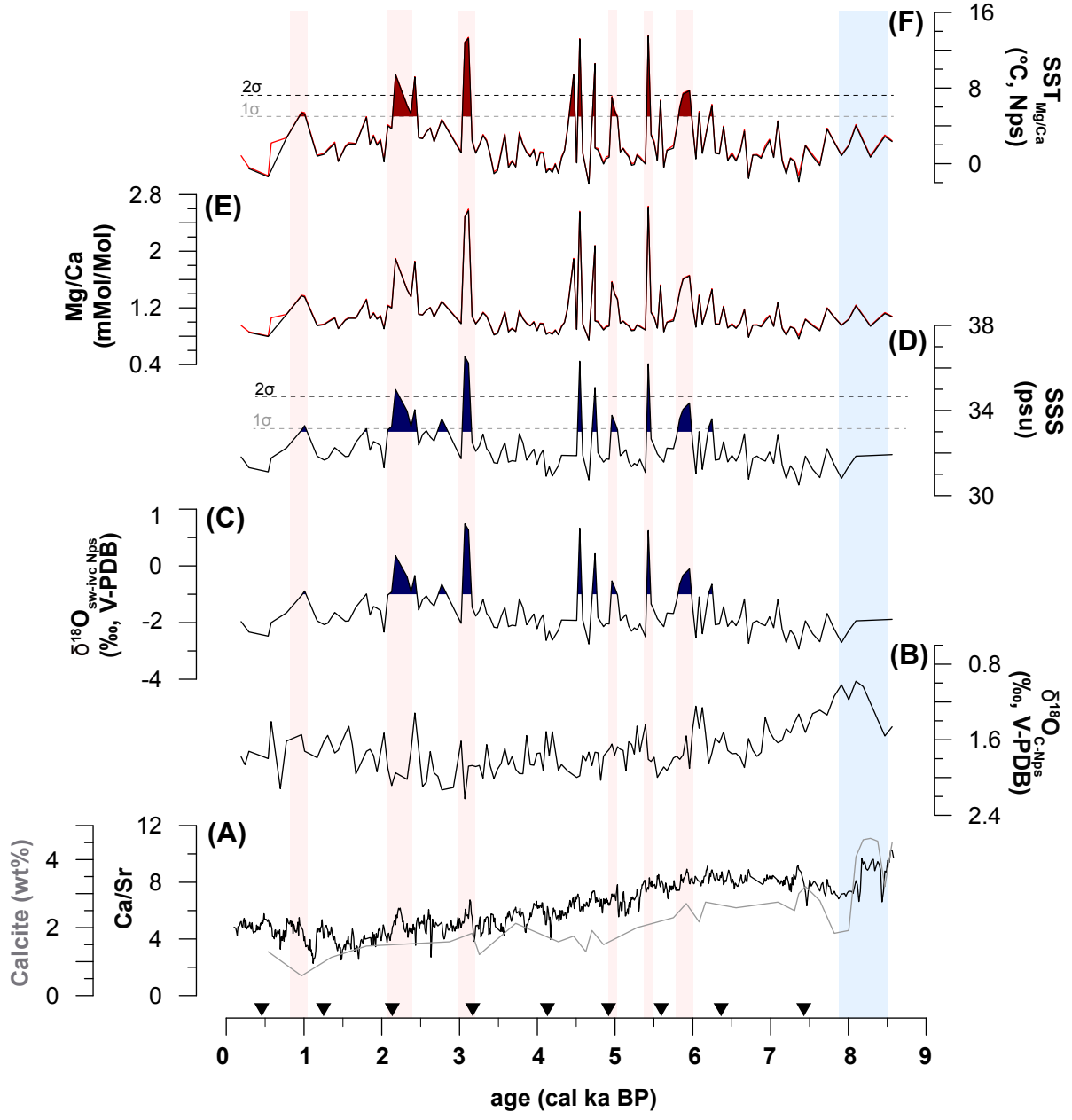

Figure 3: Results of sediment core MSM101_44-3 from St. Anns Basin. (A) Ca/Sr ratio, Calcite in weight % (wt%), (B) $\delta^{18}O$ values from planktonic foraminifer *N. pachyderma* ($\delta^{18}O_{c\text{-}Nps}$) as well as (C) ice volume corrected $\delta_{18}O$ for sea water ($\delta^{18}O_{sw\text{-}ivc}$ Nps) both in ‰, (D) calculated sea surface salinity (SSS) in psu based on LeGrande & Schmidt (2006), (E) Mg/Ca ratios from the planktonic foraminifer *N. pachydema* in mmol/mol and (F) reconstructed sea surface temperature (SST) based on Mg/Ca ratios (red line: original data; black line: corrected data) of the planktonic foraminifer *N. pachyderma* based on Jonkers et al. (2013) in °C. Inverted triangles on the x-axis indicate age points (Fig 2; Appendix A - Table A1, Matzerath et al., 2026). The blue shaded area indicates a cold phase with high freshwater input. Red shaded areas indicate warm events, linked to Gulf Stream intrusions towards the Scotian Self. Horizontal stippled lines denote the +1σ (grey) and +2σ (black) thresholds above the mean SST and SSS, defining moderate and extreme warm events.

https://doi.org/10.5194/egusphere-2026-809
Preprint. Discussion started: 17 February 2026

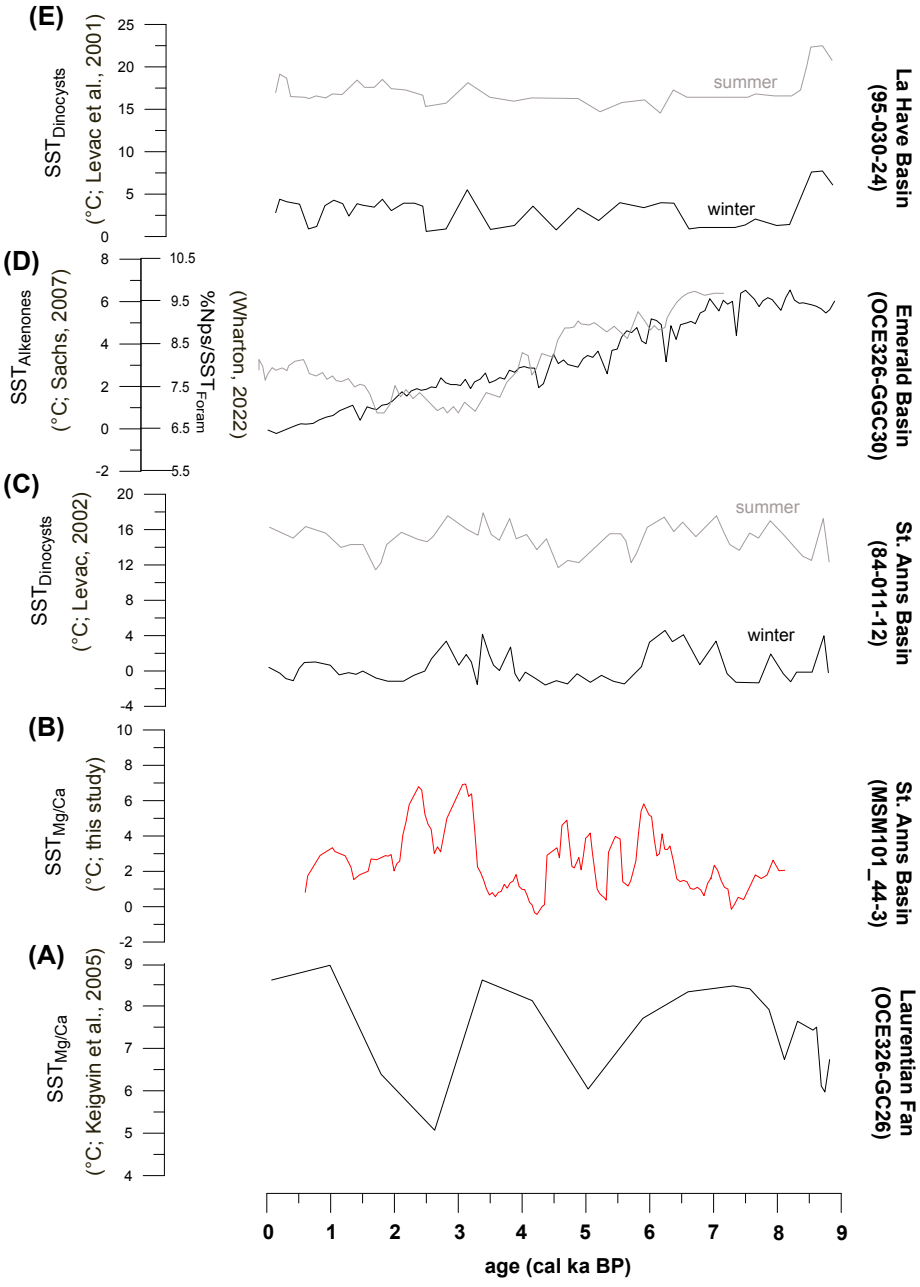

Figure 4: Comparison of Holocene sea-surface temperature (SST) reconstructions from the northwest Atlantic. (A) Mg/Ca-based SST reconstruction based on the planktonic foraminifer *N. pachyderma* from the Laurentian Fan (OCE326-26GGC; Keigwin et al. 2005). (B) Mg/Ca-based SST reconstruction from planktonic foraminifer *N. pachyderma* from the St. Anns Basin (MSM101_44-3; this study). Dinocyst-based SST reconstructions from (C) St. Anns Basin (84011-12) and (E) La Have Basin (95-030-24) representing seasonal summer and winter estimates (Levac et al. 2001; Levac, 2002). (D) Alkenone-derived SST and *N. pachyderma* reconstructed SSTs from Emerald Basin (OCE326-GGC30; Sachs, 2007; Wharton, 2022).

https://doi.org/10.5194/egusphere-2026-809
Preprint. Discussion started: 17 February 2026

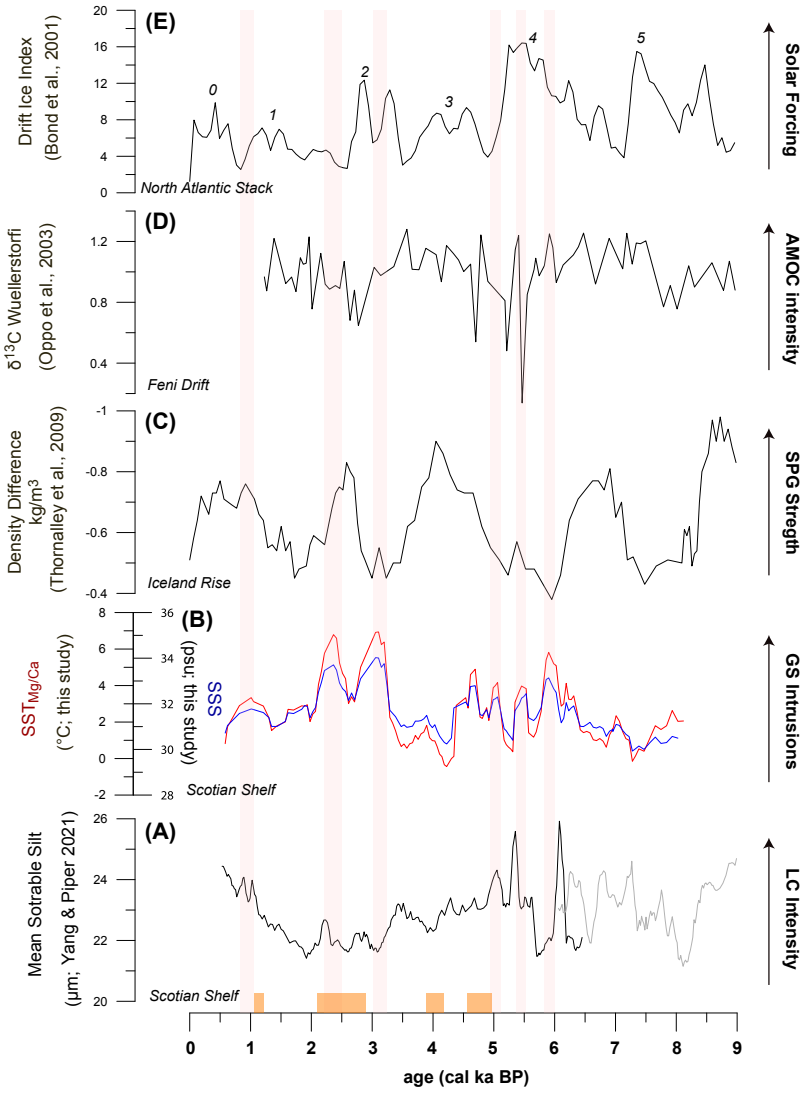

Figure 5: Comparison of Holocene oceanographic variability on the Scotian Shelf with subpolar circulation, AMOC strength, and North Atlantic climate forcing. (A) Mean sortable silt record from Emerald Basin on the Scotian Shelf, indicating LC intensity (Yang & Piper, 2021) (B) Reconstructed sea-surface temperature (SST, running average) and sea surface salinity (SSS, running average) from St. Anns Basin based on Mg/Ca rations in *N. pachyderma*. (C) East-west density gradient across the Subpolar Gyre (SPG) from (Thornalley et al., 2009). Higher density differences indicate a strong, expanded SPG and intensified Labrador Current influence; lower values reflect contracted, weak SPG conditions. (D) Benthic $\delta^{13}C$ from the subpolar North Atlantic (Oppo et al., 2003), reflecting changes in deep ventilation and Atlantic Meridional Overturing Circulation (AMOC) strength. Lower δ13C indicate reduced deep convection and a weakened AMOC. (E) North Atlantic ice-rafted debris (IRD) index representing Bond Events (Bond et al., 2001, shaded in grey). These cold subpolar intervals are characterized by enhanced drift-ice export, strong SPG circulation, and southward displacement of the Gulf Stream. Warm anomalies (shaded in red) on the Scotian Shelf indicate episodic intrusions of warm, saline Gulf Stream-sourced slope waters onto the Scotian Shelf. Orange bars indicate drought events in the U.S. (Shuman et al., 2019).

https://doi.org/10.5194/egusphere-2026-809
Preprint. Discussion started: 17 February 2026

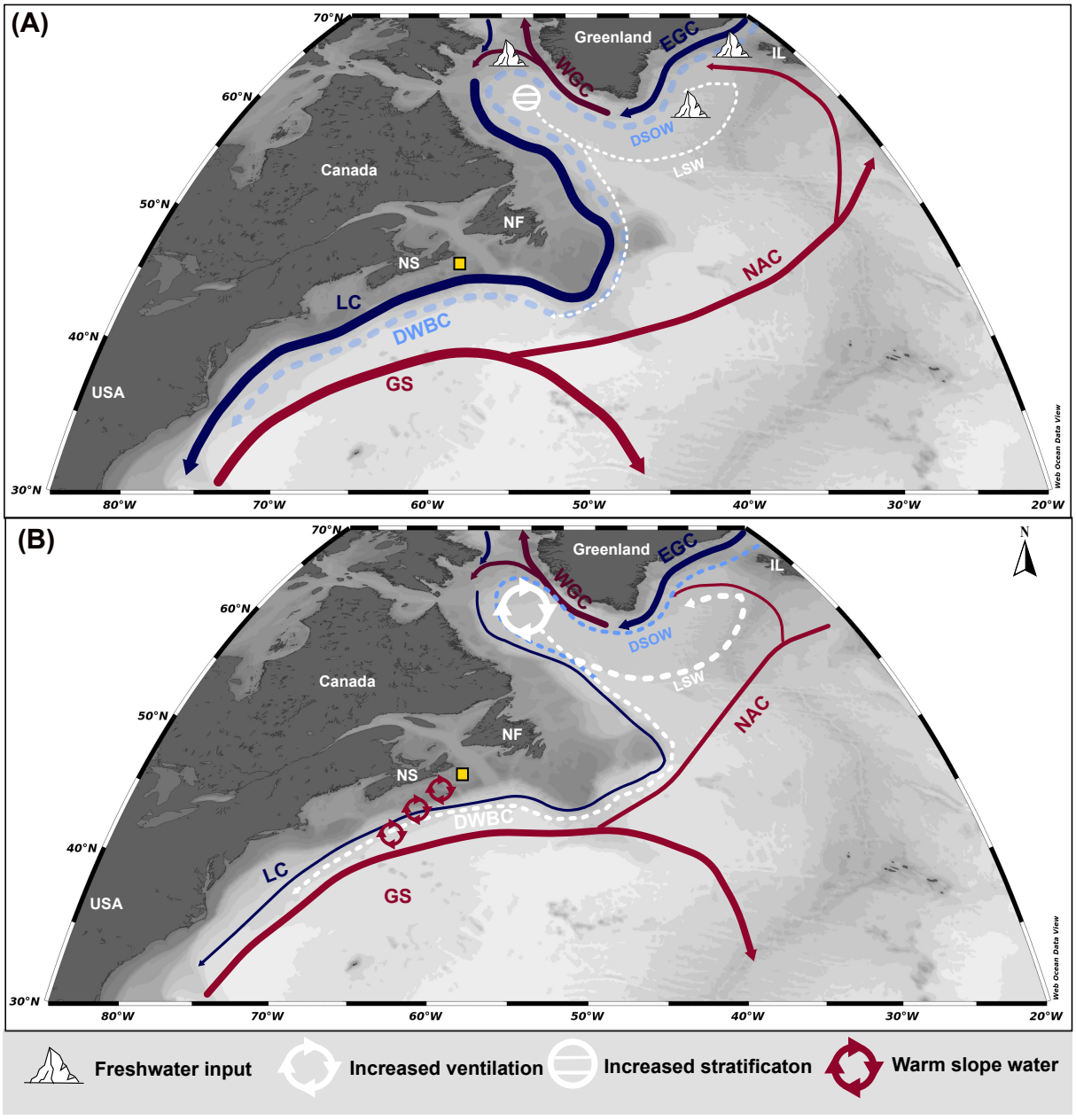

Figure 6: Conceptual model of minimum and maximum modal states circulation on the Scotian Shelf (adapted after Pickart et al., 1999). Solid arrows denote surface currents, dashed arrows denote deep currents. (A) Minimum State: Strong, onshore Labrador Current (LC) and a Denmark Strait Overflow Water (DSOW)-dominated Deep Western Boundary Current (DWBC) maintain steep density gradients across the slope and limit intrusions of warm Gulf Stream (GS) sourced waters. Increased freshwater supply (indicated by icebergs) lead to stratification in the Labrador Sea and reduced deep water production. Periods of increased freshwater supply could be related to Bond events (Bond et al., 2001). (B) Maximum State: Increased ventilation in the Labrador Sea, increased contribution of LSW to the DWBC, and a weakened LC collectively reduce density gradients across the slope, and therefore allow GS derived warmer waters to reach the Scotian Shelf. The yellow square indicates the location of this study, MSM101_44-3.

https://doi.org/10.5194/egusphere-2026-809
Preprint. Discussion started: 17 February 2026

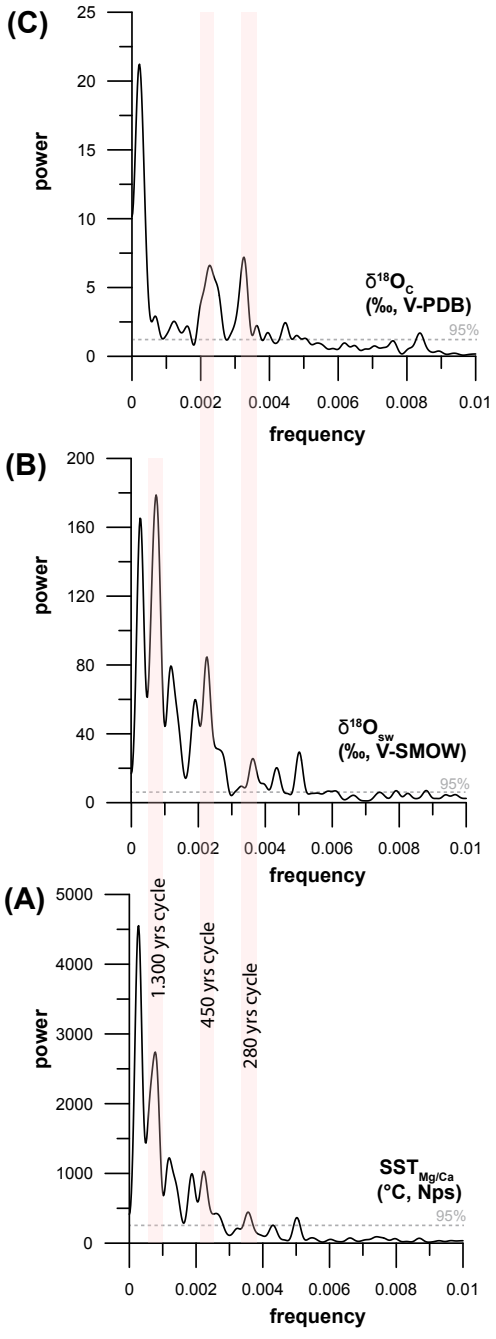

600

Figure 7: Spectral analysis of (A) sea surface temperatures based on Mg/Ca ratios in *N. pachyderma*, (B) calculated oxygen isotope variations of sea water ($\delta^{18}O_{sw}$) and (C) stable oxygen isotope variations in *N. pachyderma* ($\delta^{18}O_c$) reconstructed in sediment core MSM101_44-3. Red shaded areas indicate the most prominent frequencies and periods in our record (1.300 yrs, 450 yrs, 280 yrs). Grey horizontal stippled lines denote the 95% confidence level.

https://doi.org/10.5194/egusphere-2026-809
Preprint. Discussion started: 17 February 2026

Appendices

Appendix A

Table A1: Radiocarbon dates and calibrations from core MSM101_44-3.

Sample ID	Depth (cm)	Species	AMS ^{14}C age (^{14}C a BP)	Δ R (^{14}C yrs)	Standard deviation	Confidence interval		Age median (cal. a BP)
						from 95.4	to 94.5	
57530	26.5	mixed benthics	920±40	-86 ± 66	88	615	269	439
57531	126.5	mixed benthics	1737±29	-86 ± 66	91	1395	1022	1215
57532	226.5	mixed benthics	2540±40	-86 ± 66	116	2345	1898	2132
58011	328.5	mixed benthics	3370±35	-86 ± 66	117	3368	2908	3143
57534	426.5	mixed benthics	4110±40	-86 ± 66	124	4315	3820	4057
58013	528.5	mixed benthics	4715±40	-86 ± 66	119	5089	4598	4849
57536	627.5	mixed benthics	5290±55	-86 ± 66	111	5768	5315	5551
57537	725.5	mixed benthics	6040±40	-86 ± 66	104	6585	6164	6357
57538	826.5	mixed benthics	7040±45	-86 ± 66	93	7611	7244	7433
57539	946.5	mixed benthics	9105±50	-86 ± 66	137	9983	9455	9675

https://doi.org/10.5194/egusphere-2026-809
Preprint. Discussion started: 17 February 2026

Appendix B

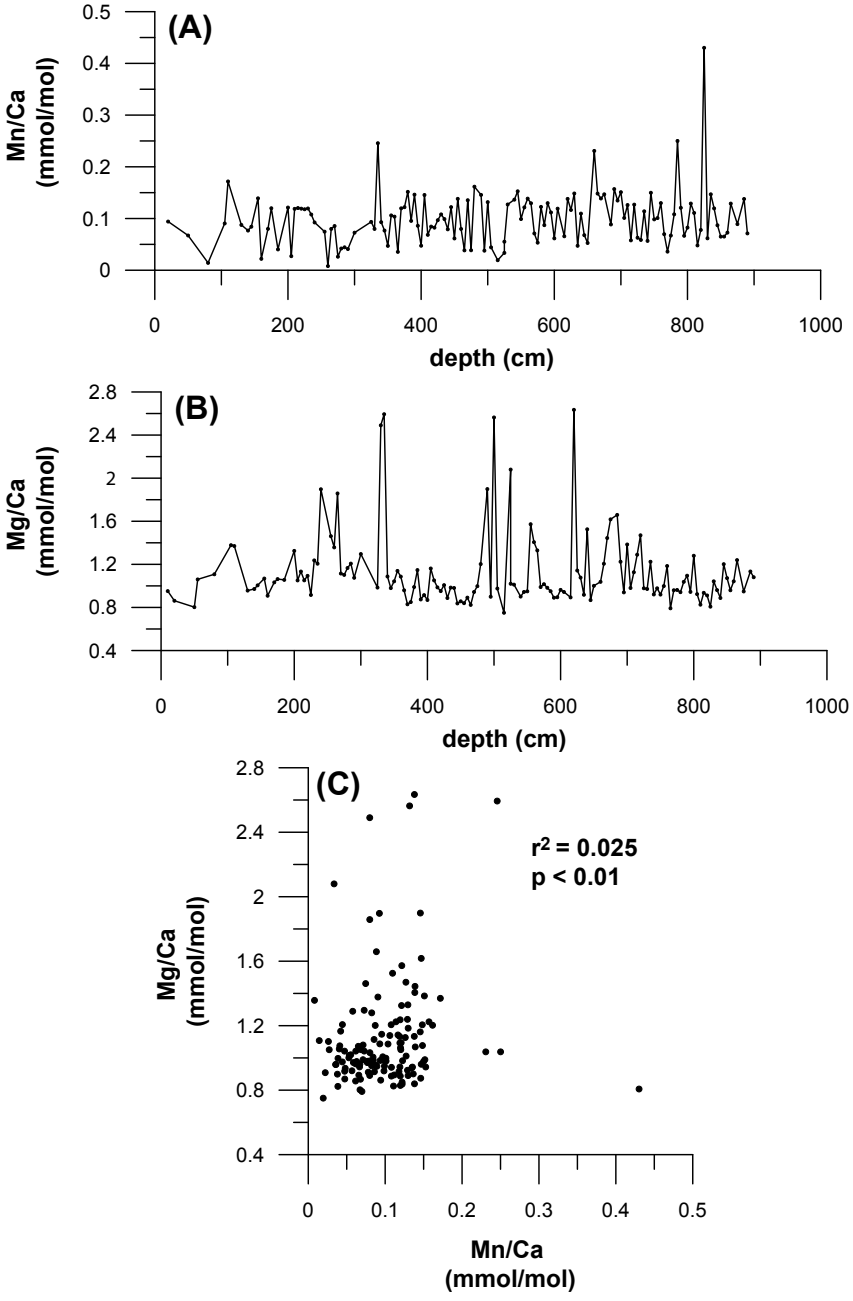

Figure B1: Downcore variability of (A) *N. pachyderma* Mn/Ca and (B) Mg/Ca rations (in mmol/mol) in core MSM101_44-3 from St. Anns Basin, Scotian Shelf. Mg/Ca values are used for sea-surface temperature (SST) reconstructions, while Mn/Ca ratios provide an indicator of post-depositional diagenetic overprinting or redox sensitive Mn mobilization. (C) Crossplot of Mg/Ca and Mn/Ca ratios (in mmol/mol) does not indicate a correlation between both ratios.

https://doi.org/10.5194/egusphere-2026-809
Preprint. Discussion started: 17 February 2026

Data availability

All data, including Ca/Sr, Calcite concentrations, Mg/Ca ratios, oxygen stable isotopes as well as calculated sea surface temperatures and sea surface salinities used for this research are available at PANGAEA – _Data Publisher for Earth & Environmental Science with Creative Commons Attribution 4.0 International license.

Mg/Ca and stable isotope data: https://doi.pangaea.de/10.1594/PANGAEA.990260

XRF and XRD data: https://doi.pangaea.de/10.1594/PANGAEA.990261

Author contributions

HK, FG and RS conducted the initial coring and field surveys in 2021. HK collected and analyzed the data, wrote the initial draft of the manuscript and prepared the figures. MK and PM contributed to data analysis and interpretation of the results. MK contributed XRD data. JG and DAF supported the Mg/Ca analyses. MK, PM, JG, SK, DAF reviewed and edited the manuscript. RS and MK acquired funding.

Competing interests

The authors declare that they have no conflict of interest

Acknowledgements

We are grateful to the captain, crew and scientific party of expedition MSM101 of RV Maria S. Merian. The work of H. Kolling was funded by the Deutsche Forschungsgemeinschaft (DFG GPF20-1-039) and the federal state of Schleswig-Holstein. We warmly thank Karen Bremer for supporting the Mg/Ca measurements, as well as Lea Morgenweck and Hanif Sulaiman for sample preparation.

Markus Kienast contributed greatly to this study. His insight and enthusiasm sustained and shaped it in lasting ways. We miss him deeply.

Financial support

Deutsche Forschungsgemeinschaft (DFG GPF20-1-039)

https://doi.org/10.5194/egusphere-2026-809
Preprint. Discussion started: 17 February 2026

References

Alley, R., & Agustsdottir, A. (2005). The 8k event: cause and consequences of a major Holocene abrupt climate change. Quaternary Science Reviews, 24(10–11), 1123–1149. https://doi.org/10.1016/j.quascirev.2004.12.004

Austermann, J., Mitrovica, J. X., Latychev, K., & Milne, G. A. (2013). Barbados-based estimate of ice volume at Last Glacial Maximum affected by subducted plate. Nature Geoscience, 6(7), 553–557. https://doi.org/10.1038/ngeo1859

Balsam, W. (1981). Late Quaternary sedimentation in the western north Atlantic: stratigraphy and paleoceanography. Palaeogeography, Palaeoclimatology, Palaeoecology, 35, 215–240. https://doi.org/10.1016/0031-0182(81)90098-5

Barker, S., Greaves, M., & Elderfield, H. (2003). A study of cleaning procedures used for foraminiferal Mg/Ca paleothermometry. Geochemistry, Geophysics, Geosystems, 4(9). https://doi.org/10.1029/2003GC000559

Bemis, B. E., Spero, H. J., Bijma, J., & Lea, D. W. (1998). Reevaluation of the oxygen isotopic composition of planktonic foraminifera: Experimental results and revised paleotemperature equations. Paleoceanography, 13(2), 150-160.

Bersch, M. (2002). North Atlantic Oscillation–induced changes of the upper layer circulation in the northern North Atlantic Ocean. Journal of Geophysical Research: Oceans, 107(C10). https://doi.org/10.1029/2001JC000901

Bond, G., Kromer, B., Beer, J., Muscheler, R., Evans, M. N., Showers, W., et al. (2001). Persistent solar influence on north atlantic climate during the Holocene. Science, 294(5549), 2130–2136. https://doi.org/10.1126/science.1065680

Born, A., & Levermann, A. (2010). The 8.2 ka event: Abrupt transition of the subpolar gyre toward a modern North Atlantic circulation. Geochemistry, Geophysics, Geosystems, 11(6). https://doi.org/10.1029/2009GC003024

Bova, S., Rosenthal, Y., Liu, Z., Godad, S. P., & Yan, M. (2021). Seasonal origin of the thermal maxima at the Holocene and the last interglacial. Nature, 589(7843), 548–553. https://doi.org/10.1038/s41586-020-03155-x

Bower, A. S., Lozier, M. S., Gary, S. F., & Böning, C. W. (2009). Interior pathways of the North Atlantic meridional overturning circulation. Nature, 459(7244), 243–247. https://doi.org/10.1038/nature07979

Boyle, E. A. (1983). Manganese carbonate overgrowths on foraminifera tests, Geochim. Cosmochim. Acta, 47, 1815–1819

Brickman, D., Hebert, D., & Wang, Z. (2018). Mechanism for the recent ocean warming events on the Scotian Shelf of eastern Canada. Continental Shelf Research, 156(December 2017), 11–22. https://doi.org/10.1016/j.csr.2018.01.001

Caesar, L., Rahmstorf, S., Robinson, A., Feulner, G., & Saba, V. (2018). Observed fingerprint of a weakening Atlantic Ocean overturning circulation. Nature, 556(7700), 191–196. https://doi.org/10.1038/s41586-018-0006-5

Colbourne, E., Holden, J., Senciall, D., Bailey, W., Craif, J., Snook, S. (2015). Physical Oceanographic conditions on the Newfoundland and Labrador Shelf during 2014. DFO Can. Sci. Advis. Sec. Res. Doc. Retrieved from https://waves-vagues.dfo-mpo.gc.ca/Library/362068.pdf

Colin, C., Frank, N., Copard, K., & Douville, E. (2010). Neodymium isotopic composition of deep-sea corals from the NE Atlantic: implications for past hydrological changes during the Holocene. Quaternary Science Reviews, 29(19–20), 2509–2517. https://doi.org/10.1016/j.quascirev.2010.05.012

https://doi.org/10.5194/egusphere-2026-809
Preprint. Discussion started: 17 February 2026

Condron, A., & Winsor, P. (2011). A subtropical fate awaited freshwater discharged from glacial Lake Agassiz. Geophysical Research Letters, 38(3), n/a-n/a. https://doi.org/10.1029/2010GL046011

deMenocal, P., Ortiz, J., Guilderson, T., & Sarnthein, M. (2000). Coherent High- and Low-Latitude Climate Variability During the Holocene Warm Period. Science, 288(5474), 2198–2202. https://doi.org/10.1126/science.288.5474.2198

Drinkwater, K. F. (1996). Atmospheric and Oceanic Variability in the Northwest Atlantic During the 1980s and Early 1990s. Journal of Northwest Atlantic Fishery Science, 18, 77–97. https://doi.org/10.2960/J.v18.a6

Dyke, A. S. (2004). An outline of North American deglaciation with emphasis on central and northern Canada (pp. 373–424). https://doi.org/10.1016/S1571-0866(04)80209-4

Elderfield, H., & Ganssen, G. (2000). Past temperature and δ18O of surface ocean waters inferred from foraminiferal Mg/Ca ratios. Nature, 405(6785), 442–445. https://doi.org/10.1038/35013033

Elderfield, H., Ferretti, P., Greaves, M., Crowhurst, S., McCave, I. N., Hodell, D., & Piotrowski, A. M. (2012). Evolution of ocean temperature and ice volume through the mid-Pleistocene climate transition. Science, 337(6095), 704–709. https://doi.org/10.1126/science.1221294

Eynaud, F., Mary, Y., Zumaque, J., Wary, M., Gasparotto, M.-C., Swingedouw, D., & Colin, C. (2018). Compiling multiproxy quantitative hydrographic data from Holocene marine archives in the North Atlantic: A way to decipher oceanic and climatic dynamics and natural modes? Global and Planetary Change, 170, 48–61. https://doi.org/10.1016/j.gloplacha.2018.07.017

Fillon, R. H. (1976). Hamilton Bank, Labrador Shelf: Postglacial sediment dynamics and paleo-oceanography. Marine Geology, 20(1), 7–25. https://doi.org/10.1016/0025-3227(76)90072-4

Fratantoni, P. S., & McCartney, M. S. (2010). Freshwater export from the Labrador Current to the North Atlantic Current at the Tail of the Grand Banks of Newfoundland. Deep-Sea Research Part I: Oceanographic Research Papers, 57(2). https://doi.org/10.1016/j.dsr.2009.11.006

Gerber, L., Lippold, J., Süfke, F. (2025). Low variability of the Atlantic Meridional Overturning Circulation throughout the Holocene. Nat Commun 16, 6748. https://doi.org/10.1038/s41467-025-61793-z

Gonçalves Neto, A., Langan, J. A., & Palter, J. B. (2021). Changes in the Gulf Stream preceded rapid warming of the Northwest Atlantic Shelf. Communications Earth and Environment, 2(1), 1–10. https://doi.org/10.1038/s43247-021-00143-5

Greco, M., Meilland, J., Zamelczyk, K., Rasmussen, T. L., & Kucera, M. (2020). The effect of an experimental decrease in salinity on the viability of the Subarctic planktonic foraminifera Neogloboquadrina incompta. Polar Research, 39. https://doi.org/10.33265/polar.v39.3842

Greene, C. H., Meyer-Gutbrod, E., Monger, B. C., McGarry, L. P., Pershing, A. J., Belkin, I. M., et al. (2013). Remote climate forcing of decadal-scale regime shifts in Northwest Atlantic shelf ecosystems. Limnology and Oceanography, 58(3), 803–816. https://doi.org/10.4319/lo.2013.58.3.0803

Heaton, T. J., Köhler, P., Butzin, M., Bard, E., Reimer, R. W., Austin, W. E. N., et al. (2020). Marine20—The Marine Radiocarbon Age Calibration Curve (0–55,000 cal BP). Radiocarbon, 62(4), 779–820. https://doi.org/10.1017/RDC.2020.68

https://doi.org/10.5194/egusphere-2026-809
Preprint. Discussion started: 17 February 2026

Hebert, D., Layton, C., Brickman, D., & Galbraith, P. S. (2021). Physical Oceanographic Conditions on the Scotian Shelf and in the Gulf of Maine during 2019. DFO Can. Sci. Advis. Sec. Res. Doc. Retrieved from http://www.dfo-mpo.gc.ca/csas-sccs/csas-sccs@dfo-mpo.gc.ca

Herbert, T. D. (2001). Review of alkenone calibrations (culture, water column, and sediments). Geochemistry, Geophysics, Geosystems, 2(2). https://doi.org/10.1029/2000GC000055

Herman, A. W., & Platt, T. (1986). Primary production profiles in the ocean-estimation from a chlorophyll light model. Oceanologica Acta, 9(1), 31-40.

Hillaire-Marcel, C., De Vernal, A., Bilodeau, G., & Weaver, A. J. (2001). Absence of deep-water formation in the Labrador Sea during the last interglacial period. Nature, 410(6832), 1073–1077. https://doi.org/10.1038/35074059

Hillaire-Marcel, C., de Vernal, A., & Piper, D. J. W. (2007). Lake Agassiz Final drainage event in the northwest North Atlantic. Geophysical Research Letters, 34(15), 1–5. https://doi.org/10.1029/2007GL030396

Hoffman, J. S., Carlson, A. E., Winsor, K., Klinkhammer, G. P., LeGrande, A. N., Andrews, J. T., & Strasser, J. C. (2012). Linking the 8.2 ka event and its freshwater forcing in the Labrador Sea. Geophysical Research Letters, 39(18). https://doi.org/10.1029/2012GL053047

Holliday, N. P., Bersch, M., Berx, B., Chafik, L., Cunningham, S., Florindo-López, C., et al. (2020). Ocean circulation causes the largest freshening event for 120 years in eastern subpolar North Atlantic. Nature Communications, 11(1), 585. https://doi.org/10.1038/s41467-020-14474-y

J.D.Haigh. (1996). The impact of solar variability on climate. Science, 272, 981.

Jennings, A., Andrews, J., Pearce, C., Wilson, L., & Ólfasdótttir, S. (2015). Detrital carbonate peaks on the Labrador shelf, a 13-7ka template for freshwater forcing from the Hudson Strait outlet of the Laurentide Ice Sheet into the subpolar gyre. Quaternary Science Reviews, 107, 62–80. https://doi.org/10.1016/j.quascirev.2014.10.022

Jetté, H., & Mott, R. J. (2007). Vegetation and Climate of Maritime Canada 6000 Years BP: A Synthesis. Géographie Physique et Quaternaire, 49(1), 141–162. https://doi.org/10.7202/033034ar

Jonkers, L., G.-J. A. Brummer, F. J. C. Peeters, H. M. van Aken, and M. F. De Jong (2010), Seasonal stratification, shell flux, and oxygen isotope dynamics of left-coiling N. pachyderma and T. quinqueloba in the western subpolar North Atlantic, Paleoceanography, 25, PA2204, doi:10.1029/2009PA001849.

Jonkers, L., Jiménez-Amat, P., Mortyn, P. G., & Brummer, G. J. A. (2013). Seasonal Mg/Ca variability of N. pachyderma (s) and G. bulloides: Implications for seawater temperature reconstruction. Earth and Planetary Science Letters, 376, 137–144. https://doi.org/10.1016/j.epsl.2013.06.019

Jutras, M., Mucci, A., Chaillou, G., Nesbitt, W. A., Wallace, D. W. R., & Hérard, O. (2022). Temporal and spatial evolution of bottom-water hypoxia in the Estuary and Gulf of St. Lawrence. EGUsphere [Preprint], (2005), 839–849.

Keigwin, L. D., & Jones, G. A. (1995). The marine record of deglaciation from the continental margin off Nova Scotia. Paleoceanography, 10(6), 973–985. https://doi.org/10.1029/95PA02643

https://doi.org/10.5194/egusphere-2026-809
Preprint. Discussion started: 17 February 2026

Keigwin, L. D., Sachs, J. P., & Rosenthal, Y. (2003). A 1600-year history of the Labrador Current off Nova Scotia. Climate Dynamics, 21(1), 53–62. https://doi.org/10.1007/s00382-003-0316-6

Keigwin, L. D., Sachs, J. P., Rosenthal, Y., & Boyle, E. A. (2005). The 8200 year B.P. event in the slope water system, western subpolar North Atlantic. Paleoceanography, 20(2), 1–14. https://doi.org/10.1029/2004PA001074

Kotov, S., Pälike, H., (2018). AGU Fall Meeting Abstracts, PP53D-1230, 2018 or https://doi.org/10.5281/zenodo.10892346

Kuroyanagi, A., & Kawahata, H. (2004). Vertical distribution of living planktonic foraminifera in the seas around Japan. Marine Micropaleontology, 53(1–2), 173–196. https://doi.org/10.1016/j.marmicro.2004.06.001

Lauzier, L. M. (1965). Long-term temperature variations in the Scotian Shelf area. ICNAF Spec. Publ, 6, 807-816.

Lazier, J. R. N., & Wright, D. G. (1993). Annual velocity variations in the Labrador Current. Journal of Physical Oceanography, 23(4). https://doi.org/10.1175/1520-0485(1993)023<0659:AVVITL>2.0.CO;2

Lea, D. W., Mashiotta, T. A., & Spero, H. J. (1999). Controls on magnesium and strontium uptake in planktonic foraminifera determined by live culturing. Geochimica et Cosmochimica Acta, 63(16), 2369–2379. https://doi.org/10.1016/S0016-7037(99)00197-0

LeGrande, A. N., & Schmidt, G. A. (2006). Global gridded data set of the oxygen isotopic composition in seawater. Geophysical Research Letters, 33(12). https://doi.org/10.1029/2006GL026011

Levac, E. (2001). High resolution Holocene palynological record from the Scotian Shelf. Marine Micropaleontology, 43(3–4), 179–197. https://doi.org/10.1016/S0377-8398(01)00033-0

Levac, E. (2002). High Resolution Palynological Records From Atlantic Canada: Regional Holocene Paleoceanographic and Paleoclimatic History, (May).

Levac, E., De Vernal, A., & Blake, W. (2001). Sea-surface conditions in northernmost Baffin Bay during the Holocene: Palynological evidence. Journal of Quaternary Science, 16(4), 353–363. https://doi.org/10.1002/jqs.614

Levac, E., Lewis, C. F. M., & Miller, A. A. L. (2011). The impact of the final Lake Agassiz flood recorded in Northeast Newfoundland and Northern Scotian shelves based on century-scale palynological data. Geophysical Monograph Series, 193(1), 139–159. https://doi.org/10.1029/2010GM001051

Licciardi, J. M., Teller, J. T., & Clark, P. U. (1999). Freshwater routing by the Laurentide Ice Sheet during the last deglaciation (pp. 177–201). https://doi.org/10.1029/GM112p0177

Locarnini, R.A., A.V. Mishonov, O.K. Baranova, J.R. Reagan, T.P. Boyer, D. Seidov, Z. Wang, H.E. Garcia, C. Bouchard, S.L. Cross, C.R. Paver, and D. Dukhovskoy. World Ocean Atlas 2023, Volume 1: Temperature. A. Mishonov Technical Ed. NOAA Atlas NESDIS 89, doi.org/10.25923/54bh-1613

Lochte, A. A., Repschläger, J., Kienast, M., Garbe-Schönberg, D., Andersen, N., Hamann, C., & Schneider, R. (2019). Labrador Sea freshening at 8.5 ka BP caused by Hudson Bay Ice Saddle collapse. Nature Communications, 10(1), 1–9. https://doi.org/10.1038/s41467-019-08408-6

Loder, John W.; Petrie, Brian; Gawarkiewicz, G. (1998). The coastal ocean off northeastern North America: a large-scale view. The Sea, 11(JANUARY 1998), 105–133.

https://doi.org/10.5194/egusphere-2026-809
Preprint. Discussion started: 17 February 2026

Loder, J. W., Hannah, C. G., Petrie, B. D., & Gonzalez, E. A. (2003). Hydrographic and transport variability on the Halifax section. Journal of Geophysical Research: Oceans, 108(C11). https://doi.org/10.1029/2001JC001267

Loring, D. H., & Nota, D. J. G. (1973). Bulletin of the Fisheries Research Board of Canada Morphology and Sediments et Gull of St . Lawrence Board of Canada morphology and sediments.

Marsh, R., Petie, B., Weidman, C. R., Dickson, R. R., Loder, J. W., Hannah, C. G., et al. (1999). The 1882 tilefish kill — a cold event in shelf waters off the north-eastern United States? Fisheries Oceanography, 8(1), 39–49. https://doi.org/10.1046/j.1365-2419.1999.00092.x

Marsicek, J., Shuman, B. N., Bartlein, P. J., Shafer, S. L., & Brewer, S. (2018). Reconciling divergent trends and millennial variations in Holocene temperatures. Nature, 554(7690), 92–96. https://doi.org/10.1038/nature25464

Matzerath, P., Kolling, H. M., Kienast, M., Fahl, K., Stein, R., Gross, F., & Schneider, R. R. (2026). Holocene sea-ice and productivity changes on the Scotian Shelf , NW Atlantic. Quaternary Science Reviews, 372(November 2025), 109694. https://doi.org/10.1016/j.quascirev.2025.109694

McNeely, R., Dyke, A. S., & Southon, J. R. (2006). Canadian marine reservoir ages, preliminary data assessment. https://doi.org/10.4095/221564

Moffa-Sánchez, P., & Hall, I. R. (2017). North Atlantic variability and its links to European climate over the last 3000 years. Nature Communications, 8(1), 1726. https://doi.org/10.1038/s41467-017-01884-8

Moffa-Sánchez, Paola, Born, A., Hall, I. R., Thornalley, D. J. R., & Barker, S. (2014). Solar forcing of North Atlantic surface temperature and salinity over the past millennium. Nature Geoscience, 7(4), 275–278. https://doi.org/10.1038/ngeo2094

Morison, J., Kwok, R., Peralta-Ferriz, C., Alkire, M., Rigor, I., Andersen, R., & Steele, M. (2012). Changing Arctic Ocean freshwater pathways. Nature, 481(7379), 66–70. https://doi.org/10.1038/nature10705

Müller, P. J., Kirst, G., Ruhland, G., von Storch, I., & Rosell-Melé, A. (1998). Calibration of the alkenone paleotemperature index U37K′ based on core-tops from the eastern South Atlantic and the global ocean (60°N-60°S). Geochimica et Cosmochimica Acta, 62(10), 1757–1772. https://doi.org/10.1016/S0016-7037(98)00097-0

Muscheler R., Beer J., Kromer B. (2003), Long-term climate variations and solar effects.Processing in ISCS Symposium, "Solar Variability as an Input to the Earth's Environment", SP-535, ESA

New, A. L., Smeed, D. A., Czaja, A., Blaker, A. T., Mecking, J. V., Mathews, J. P., & Sanchez-Franks, A. (2021). Labrador Slope Water connects the subarctic with the Gulf Stream. Environmental Research Letters, 16(8). https://doi.org/10.1088/1748-9326/ac1293

Nürnberg, D., Bijma, J., & Hemleben, C. (1996). Assessing the reliability of magnesium in foraminiferal calcite as a proxy for water mass temperatures. Geochimica et Cosmochimica Acta, 60(5), 803–814. https://doi.org/10.1016/0016-7037(95)00446-7

Oppo, D. W., McManus, J. F., & Cullen, J. L. (2003). Deepwater variability in the Holocene epoch. Nature, 422(6929), 277–277. https://doi.org/10.1038/422277b

https://doi.org/10.5194/egusphere-2026-809
Preprint. Discussion started: 17 February 2026

Orme, L. C., Miettinen, A., Seidenkrantz, M. S., Tuominen, K., Pearce, C., Divine, D. V., et al. (2021). Mid to late-Holocene sea-surface temperature variability off north-eastern Newfoundland and its linkage to the North Atlantic Oscillation. Holocene, 31(1), 3–15. https://doi.org/10.1177/0959683620961488

Osman, M. B., Tierney, J. E., Zhu, J., Tardif, R., Hakim, G. J., King, J., & Poulsen, C. J. (2021). Globally resolved surface temperatures since the Last Glacial Maximum. Nature, 599(7884), 239–244. https://doi.org/10.1038/s41586-021-03984-4

Pershing, A. J., Alexander, M. A., Hernandez, C. M., Kerr, L. A., Bris, A. Le, Mills, K. E., et al. (2016). Response to comments on "Slow adaptation in the face of rapid warming leads to collapse of the Gulf of Maine cod fishery. Science, 352(6284), 423. https://doi.org/10.1126/science.aae0463

Peterson, I., Greenan, B., Gilbert, D., & Hebert, D. (2017). Variability and wind forcing of ocean temperature and thermal fronts in the <scp>S</scp> lope <scp>W</scp> ater region of the <scp>N</scp> orthwest <scp>A</scp> tlantic. Journal of Geophysical Research: Oceans, 122(9), 7325–7343. https://doi.org/10.1002/2017JC012788

Petrie, B. (2007). Does the North Atlantic Oscillation affect hydrographic properties on the Canadian Atlantic Continental Shelf? Atmosphere - Ocean, 45(3), 141–151. https://doi.org/10.3137/ao.450302

Petrie, B., & Drinkwater, K. (1993). Temperature and salinity variability on the Scotian Shelf and in the Gulf of Maine 1945–1990. Journal of Geophysical Research: Oceans, 98(C11), 20079–20089. https://doi.org/10.1029/93JC02191

Petrie, B., & Yeats, P. (2000). Annual and interannual variability of nutrients and their estimated fluxes in the Scotian Shelf - Gulf of Maine region. Canadian Journal of Fisheries and Aquatic Sciences, 57(12), 2536–2546. https://doi.org/10.1139/f00-235

Pickart, R. S., McKee, T. K., Torres, D. J., & Harrington, S. A. (1999). Mean structure and interannual variability of the slopewater system south of Newfoundland. Journal of Physical Oceanography, 29(10), 2541–2558. https://doi.org/10.1175/1520-0485(1999)029<2541:MSAIVO>2.0.CO;2

Piper, D. J. W., Li, G., Andrews, J. T., Jennings, A. E., & Robertson, L. (2021). Transport of fine-grained sediment in oceanic currents: Holocene supply to sediment drifts around Flemish Cap by the Labrador Current. Marine Geology, 436(December 2020), 106494. https://doi.org/10.1016/j.margeo.2021.106494

Ramsey, C. B. (2008). Deposition models for chronological records. Quaternary Science Reviews, 27(1–2), 42–60. https://doi.org/10.1016/j.quascirev.2007.01.019

Ramsey, C., B. (2009). Bayesian Analysis of Radiocarbon Dates. Radiocarbon, 51(1), 337–360. https://doi.org/10.1017/S0033822200033865

Renkl, C., Oliver, E.C.J. & Thompson, K.R. (2024). Downscaling the ocean response to the Madden–Julian Oscillation in the Northwest Atlantic and adjacent shelf seas. Clim Dyn 62, 6719–6744. https://doi.org/10.1007/s00382-024-07233-y

Rashid, H., Piper, D. J. W., Lazar, K. B., McDonald, K., & Saint-Ange, F. (2017). The Holocene Labrador Current: Changing linkages to atmospheric and oceanographic forcing factors. Paleoceanography, 32(5), 498–510. https://doi.org/10.1002/2016PA003051

https://doi.org/10.5194/egusphere-2026-809
Preprint. Discussion started: 17 February 2026

Reagan, J.R., D. Seidov, Z. Wang, D. Dukhovskoy, T.P. Boyer, R.A. Locarnini, O.K. Baranova, A.V. Mishonov, H.E. Garcia, C. Bouchard, S.L. Cross, and C.R. Paver. World Ocean Atlas 2023, Volume 2: Salinity. A. Mishonov, Technical Editor, NOAA Atlas NESDIS 90, doi.org/10.25923/70qt-9574

Richter, T. O., van der Gaast, S., Koster, B., Vaars, A., Gieles, R., de Stigter, H. C., et al. (2006). The Avaatech XRF Core Scanner: technical description and applications to NE Atlantic sediments. Geological Society, London, Special Publications, 267(1), 39–50. https://doi.org/10.1144/GSL.SP.2006.267.01.03

Rohling, E. J., & Pälike, H. (2005). Centennial-scale climate cooling with a sudden cold event around 8,200 years ago. Nature, 434(7036), 975–979. https://doi.org/10.1038/nature03421

Saba, V. S., Griffies, S. M., Anderson, W. G., Winton, M., Alexander, M. A., Delworth, T. L., Hare, J. A., Harrison, M., J., Rosati, A., Vecchi, G. A., Zhang, R. (2016). Enhanced warming of Northwest Atlantic Ocean under climate change. Journal of Geophysical Research: Oceans, 121, 118–132. https://doi.org/10.1002/2015JC011346.Received

Sachs, J. P. (2007). Cooling of Northwest Atlantic slope waters during the Holocene. Geophysical Research Letters, 34(3), 1–4. https://doi.org/10.1029/2006GL028495

Schneider, B., Leduc, G., & Park, W. (2010). Disentangling seasonal signals in Holocene climate trends by satellite-model-proxy integration. Paleoceanography, 25(4), 1–13. https://doi.org/10.1029/2009PA001893

Schneider, R., Brembach, K., Gößling, P., Groß, F., Heinrich, S., Huygen, F., et al. (2021). Paleoclimate and Biogeochemistry Nova Scotia Margin Cruise No. MSM101. Maria S. Merian Berichte. https://doi.org/10.48433/cr_msm101

Scott, D. B., Mudie, P. J., Vilks, G., & Younger, D. C. (1984). Latest Pleistocene—Holocene paleoceanographic trends on the continental margin of eastern Canada: Foraminiferal, dinoflagellate and pollen evidence. Marine Micropaleontology, 9(3). https://doi.org/10.1016/0377-8398(84)90013-6

Seidov, D., Mishonov, A., & Parsons, R. (2021). Recent warming and decadal variability of Gulf of Maine and Slope Water. Limnology and Oceanography, 66(9), 3472–3488. https://doi.org/10.1002/lno.11892

Sheldon, C. M., Seidenkrantz, M. S., Pearce, C., Kuijpers, A., Hansen, M. J., & Christensen, E. Z. (2016). Holocene oceanographic changes in SW Labrador Sea, off Newfoundland. Holocene, 26(2), 274–289. https://doi.org/10.1177/0959683615608690

Shuman, B. N., Marsicek, J., Oswald, W. W., & Foster, D. R. (2019). Predictable hydrological and ecological responses to Holocene North Atlantic variability. Proceedings of the National Academy of Sciences of the United States of America, 116(13), 5985–5990. https://doi.org/10.1073/pnas.1814307116

Siddall, M., Rohling, E. J., Almogi-Labin, A., Hemleben, C., Meischner, D., Schmelzer, I., & Smeed, D. A. (2003). Sea-level fluctuations during the last glacial cycle. Nature, 423(6942), 853–858. https://doi.org/10.1038/nature01690

Silver, A., Gangopadhyay, A., Gawarkiewicz, G., Fratantoni, P., & Clark, J. (2023). Increased gulf stream warm core ring formations contributes to an observed increase in salinity maximum intrusions on the Northeast Shelf. Scientific Reports, 13(1), 7538. https://doi.org/10.1038/s41598-023-34494-0

https://doi.org/10.5194/egusphere-2026-809
Preprint. Discussion started: 17 February 2026

Simstich, J., Sarnthein, M., & Erlenkeuser, H. (2003). Paired δ18O signals of Neogloboquadrina pachyderma (s) and Turborotalita quinqueloba show thermal stratification structure in Nordic Seas. Marine Micropaleontology, 48(1–2), 107–125. https://doi.org/10.1016/S0377-8398(02)00165-2

Solignac, S., De Vernal, A., & Hillaire-Marcel, C. (2004). Holocene sea-surface conditions in the North Atlantic - Contrasted trends and regimes in the western and eastern sectors (Labrador Sea vs. Iceland Basin). Quaternary Science Reviews, 23(3–4), 319–334. https://doi.org/10.1016/j.quascirev.2003.06.003

Solignac, S., Seidenkrantz, M.-S., Jessen, C., Kuijpers, A., Gunvald, A. K., & Olsen, J. (2011). Late-Holocene sea-surface conditions offshore Newfoundland based on dinoflagellate cysts. The Holocene, 21(4), 539–552. https://doi.org/10.1177/0959683610385720

Spooner, I., Douglas, M. S. V., & Terrusi, L. (2002). Multiproxy evidence of an early Holocene (8.2 kyr) climate oscillation in central Nova Scotia, Canada. Journal of Quaternary Science, 17(7), 639–645. https://doi.org/10.1002/jqs.716

Staines-Urías, F., Kuijpers, A., & Korte, C. (2013). Evolution of subpolar North Atlantic surface circulation since the early Holocene inferred from planktic foraminifera faunal and stable isotope records. Quaternary Science Reviews, 76, 66–81. https://doi.org/10.1016/j.quascirev.2013.06.016

Straneo, F., & Saucier, F. (2008). The outflow from Hudson Strait and its contribution to the Labrador Current. Deep Sea Research Part I: Oceanographic Research Papers, 55(8), 926–946. https://doi.org/10.1016/j.dsr.2008.03.012

Swingedouw, D., Terray, L., Cassou, C., Voldoire, A., Salas-Mélia, D., & Servonnat, J. (2011). Natural forcing of climate during the last millennium: fingerprint of solar variability. Climate Dynamics, 36(7–8), 1349–1364. https://doi.org/10.1007/s00382-010-0803-5

Thomas, E. R., Wolff, E. W., Mulvaney, R., Steffensen, J. P., Johnsen, S. J., Arrowsmith, C., et al. (2007). The 8.2 ka event from Greenland ice cores. Quaternary Science Reviews, 26(1–2). https://doi.org/10.1016/j.quascirev.2006.07.017

Thornalley, D. J. R., Elderfield, H., & McCave, I. N. (2009). Holocene oscillations in temperature and salinity of the surface subpolar North Atlantic. Nature, 457(7230), 711–714. https://doi.org/10.1038/nature07717

Townsend, D. W., Pettigrew, N. R., Thomas, M. A., Neary, M. G., McGillicuddy, D. J., & O'Donnell, J. (2015). Water masses and nutrient sources to the Gulf of Maine. Journal of Marine Research, 73(3–4), 93–122. https://doi.org/10.1357/002224015815848811

Vacchi, M., Engelhart, S. E., Nikitina, D., Ashe, E. L., Peltier, W. R., Roy, K., et al. (2018). Postglacial relative sea-level histories along the eastern Canadian coastline. Quaternary Science Reviews, 201, 124–146. https://doi.org/10.1016/j.quascirev.2018.09.043

Vasil'ev S.S., Dergachev V.A., Raspopov O.M. Sources of the long-term variations of the radiocarbon concentration in the Earth's atmosphere. Geomagnetism and Aeronomy, 39 (1999), pp. 80-89

de Vernal, A., & Hillaire-Marcel, C. (2008). Natural Variability of Greenland Climate, Vegetation, and Ice Volume During the Past Million Years. Science, 320(5883), 1622–1625. https://doi.org/10.1126/science.1153929

https://doi.org/10.5194/egusphere-2026-809
Preprint. Discussion started: 17 February 2026

de Vernal, Anne, & Hillaire-Marcel, C. (2006). Provincialism in trends and high frequency changes in the northwest North Atlantic during the Holocene. Global and Planetary Change, 54(3–4), 263–290. https://doi.org/10.1016/j.gloplacha.2006.06.023

Vilks, G., & Rashid, M. A. (1976). Post-glacial paleo-oceanography of Emerald Basin, Scotian Shelf. Canadian Journal of Earth Sciences, 13(9), 1256–1267. https://doi.org/10.1139/e76-128

Wanamaker, A. D., Kreutz, K. J., Schöne, B. R., Pettigrew, N., Borns, H. W., Introne, D. S., et al. (2008). Coupled North Atlantic slope water forcing on Gulf of Maine temperatures over the past millennium. Climate Dynamics, 31(2–3), 183–194. https://doi.org/10.1007/s00382-007-0344-8

Wharton, J. (2022). Thermal structure of the Northwest Atlantic during the last 25,000 years. Dissertation, University College, London, 1–335. accessed via: https://discovery.ucl.ac.uk/id/eprint/10164435/

Willard, D. A., Bernhardt, C. E., Korejwo, D. A., & Meyers, S. R. (2005). Impact of millennial-scale Holocene climate variability on eastern North American terrestrial ecosystems: Pollen-based climatic reconstruction. Global and Planetary Change, 47(1), 17–35. https://doi.org/10.1016/j.gloplacha.2004.11.017

Yang, Y., & Piper, D. J. W. (2021). Alongflow variability of the Labrador Current during the Holocene. Quaternary Science Reviews, 267, 107110. https://doi.org/10.1016/j.quascirev.2021.107110

Zhang, R. (2008). Coherent surface-subsurface fingerprint of the Atlantic meridional overturning circulation. Geophysical Research Letters, 35(20). https://doi.org/10.1029/2008GL035463

Zhang, R., & Vallis, G. K. (2007). The Role of Bottom Vortex Stretching on the Path of the North Atlantic Western Boundary Current and on the Northern Recirculation Gyre. Journal of Physical Oceanography, 37(8), 2053–2080. https://doi.org/10.1175/JPO3102.1